

Combining geology, geomorphology and geotechnical data for a safer urban extension: Application to the Antananarivo capital city (Madagascar)



Solofo Nirina Andriamamonjisoa^a, Aurélia Hubert-Ferrari^{b,*}

^a University of Antananarivo, Department of Earth Sciences, Geotechnical Laboratory, B.P 906 - 101, Antananarivo, Madagascar

^b Department of Geography, University of Liège, allée du 6 août 2, 4000, Liège, Belgium

ARTICLE INFO

Keywords:

Antananarivo
Engineering geological mapping
Geotechnical underground data
Construction
Urban geology
Geomorphology
GIS technics
Soil bearing capacity

ABSTRACT

Metropolitan and suburban areas in Africa are rapidly expanding with, in general, a poor safe urban management. Urban development in zones not suitable for construction leads to significant economic loss. The aggregate building damage combined with other environmental treats like drought, flooding or landsliding are enhancing African city vulnerability. Simple cartographic products made available to the general public could facilitate the first stage of planning and management considering parameters that affect building foundation. We combine here in ARCGIS geological, geomorphological and geotechnical data to provide such a framework focusing on the capital city of Antananarivo in Madagascar. The city was initially constructed on basement hills covered with a thick loose weathered layer and is expanding into the alluvial lowland watered by the Ikopa River. About 221 boreholes with pressumeters and laboratory data provide a picture of the underground characteristics, and allow the computation of the soil bearing capacity, the key parameter we used to assess building suitability. Lithology, slope, land-use and ground water level are combine to build a first geotechnical map that is completed using a mapping of the soil bearing capacity combined with land-use and geohydrological constraints. The geotechnical maps divide the city into zones with different constructive conditions that can be use as a first tool for urban development planning.

1. Introduction

During the last 40 years, the population in Africa has nearly triple reaching more than 1.2 billions inhabitants and is expected to double in the next 30 years. The population growth, which is in excess of 2% every year, is paired with a general migration from rural to suburban areas. Presently a majority of the African population is still leaving in the countryside, but Africa is experiencing a rapid urban growth (UNDESA/PD, 2012; Cobbinah, 2015). The fast and often uncontrolled urbanization is a challenge particularly in Africa, where underground stability is an issue given (1) the thick lateritic cover called here regolith resulting from a deep chemical weathering (e.g. Thomas, 1994), and (2) the high rainfall intensity resulting in flooding (e.g. Douglas et al., 2008), landsliding (e.g. Jacobs et al., 2016), gullying (e.g. Lateef et al., 2010) and unstable foundations (e.g. Shaaban et al., 2013). These two characteristics are specific to tropical regions. Uncontrolled, unsafe and non-sustainable urbanization is a problem particularly acute in Madagascar, which ranks first in the World Risk Index regarding the probability to sustain damages related to natural hazards (Rakototsimba and Bettencourt, 2010; Bündnis Entwicklung Hilft and

United Nations University, 2016). During the rainy season from October to April, average rainfall ranges from 1200 to 1500 mm/yr (Jury, 2003), and most of the heavy precipitation is concentrated during tropical cyclones striking regularly the island (Nash et al., 2015). During hurricane seasons, flooding, landsliding (Mietton and Razafimahefa, 2011) and soil erosion (Tricart, 1953; Cox et al., 2010) are widespread and strongly affect the population (Clayton, 2012; Peyrusaubes, 2016). The resulting economic damages can be considerable (Bureau National de Gestion des Risques et des Catastrophes, 2015). For example, in January 2015 the CHEDZA cyclone heavily stroke the capital city of Antananarivo after the island had already experienced heavy rainfall. The cyclone damaged the main water pumps and triggered widespread flooding and landsliding. About 80 people were killed and damages reached about \$40 million (2015 USD), 0.4% of the PIB. In 2017, natural disasters (tropical cyclone and drought) did cost \$400 millions de dollars (4% of GDP) to Madagascar.

According to the database of the urban municipality of Antananarivo and the National Institute of Statistics (INSTAT), the capital Antananarivo, in the region of Analamanga, counts ~1.3 millions inhabitants and covers over an administrative-limits area of 86.4 km²

* Corresponding author. Department of Geography, University of Liège, allée du 6 août 2, 4000, Liège, Belgium.
E-mail address: aurelia.ferrari@uliege.be (A. Hubert-Ferrari).

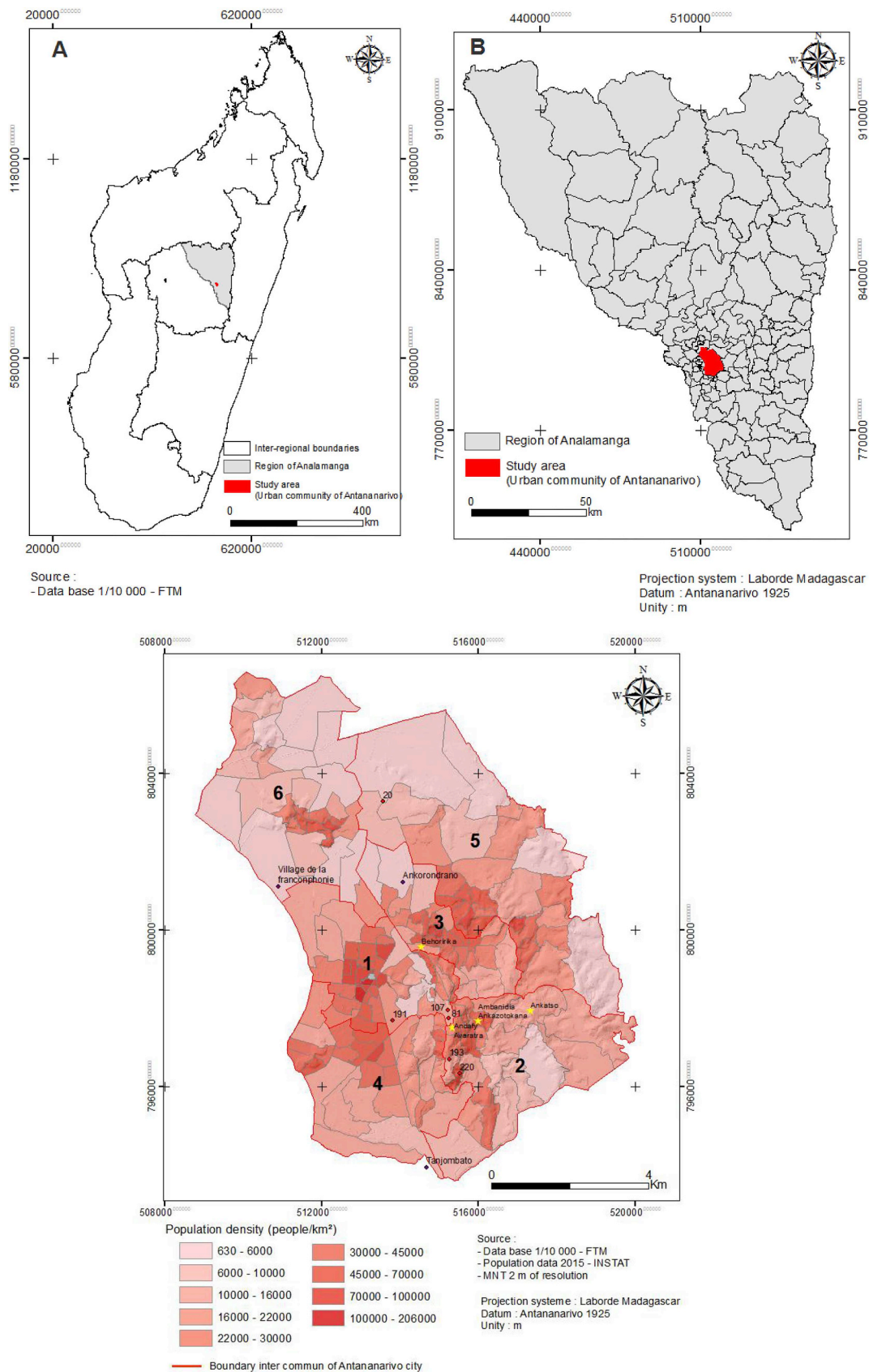


Fig. 1. Antananarivo location, population and infrastructure. A. Administrative division in provinces in Madagascar; B. Administrative division in districts in the Analamanga province; C. Density of population and administrative boundaries in urban city of Antananarivo. 1:1st district, 2: 2nd district, 3: 3rd district, 4: 4th district, 5: 5th district, 6: 6th district; D. Density of building and road system in the city of Antananarivo. Specific locations mentioned in the text are indicated (Lapan'ny tovolahy, Ambohimitsimbina, Lycée Maria Manjaka, Village de la francophonie, Ankorondrano, Tanjombato).

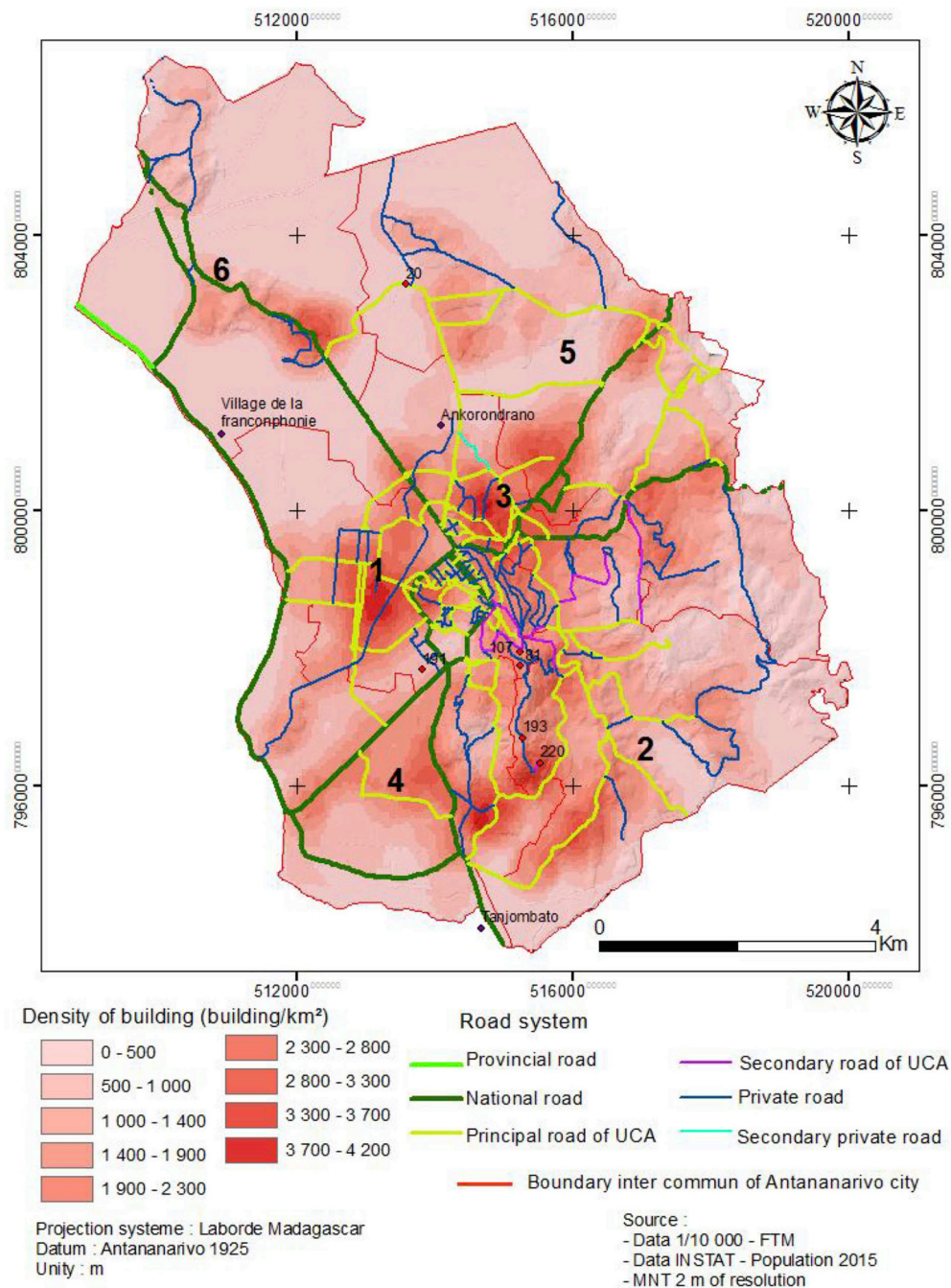


Fig. 1. (continued)

(Fig. 1). It represents 30% of the urban population in Madagascar and 30% of the national GDP (Rabe, 2012). In this rapidly expanding city, the urban planning management is increasingly challenging given the growing need for building and infrastructures to support an expanding urban population. The capital Antananarivo is facing a main recurring problems regarding building construction linked to a poor knowledge of the underground geotechnical characteristics and thus inadequate dimensioning calculation for building foundation. No study is generally available on the topics and available to the general public. Recurring problem occurs in connection with the type of building foundation, the underground characteristics and human error or carelessness as illustrated in Fig. 2.

To tackle the challenges of an increasing urbanization in the specific context of the Antananarivo area, we combine geology, geomorphology, hydrogeology, land-use and a geotechnical borehole data to

build semi-quantitative geotechnical maps of the capital. Such maps are the first step for a safer urban development. Geotechnical mapping was developed in the 1950's in Czechoslovakia (Peter, 1969), and it was more recently applied in Africa, for example, in Egypt (Aly et al., 2015), in Morocco (Lemacha et al., 2017), in Congo (Lateef et al., 2010), in South Africa (e.g. Richards, 2000), in Tunisia (El May et al., 2010), and in Ethiopia (e.g. Berhane et al., 2013).

In the present study, we first expose the data set and methods used in the following. We then outline key characteristics of the Antananarivo area: its geomorphology and geology, its urban characteristics and its hydrogeology. Then we analyze the available borehole database to outline the typical underground lithological and geotechnical characteristics of the Antananarivo area. We finally present two cartographic products that include the geotechnical data and can be used for urban planning. The first one is based on an homogeneous

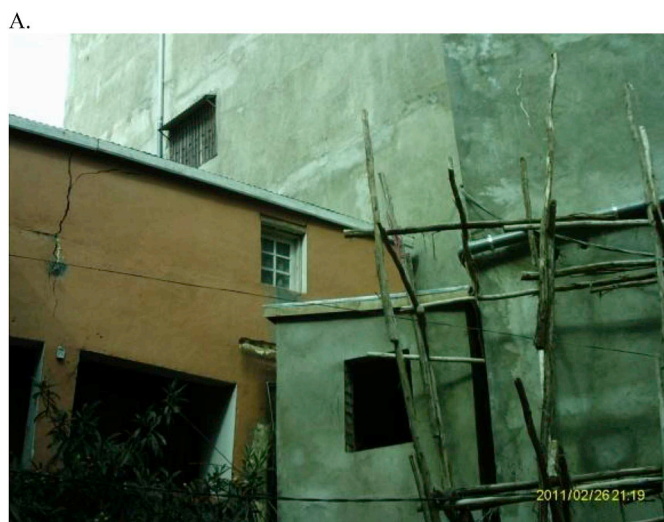


Fig. 2. A. Fissuring on the environment building induced by the construction of a 7 floors building in Behoririka (location cf. Fig. 1-C). B. Fissuring in relation to a punching failure in the foundation of a 3 floors building in Ambanidia-Ankazotokana (location cf. Fig. 1-C).

data, i.e lithology and slopes to define units with specific geotechnical characteristics; the second one is directly based on the spatially inhomogeneous geotechnical data set aggregated vertically by the computation of the soil bearing capacity. On the two maps, information relative to ground water levels is indicated, as a shallow water ($< 1\text{m}$) is not suitable for building construction. The limitation and potential of engineering geological maps obtained are finally discussed.

2. Material and methods

2.1. Urban data

In the present study, the urban data set we used regarding the road network and building (Fig. 1D) was provided by the Institut Géographique et Hydrographique de Madagascar (FTM). The original data set scale is 1/10 000. This data was used in conjunction with the 2015 population census by municipality (i.e. Fokomtany) (Fig. 1C) made available by the Institut National de la Statistique (INSTAT).

2.2. Topography, land cover and geology

We used a digital elevation model of 2 m resolution of the capital

city (Fig. 3) derived from Pleiade images acquired by the project entitled Gestion du Risque Inondation et Mouvement de Terrain à Antananarivo (GRIMA) of the Region Réunion funded by the European Program called CTE OCEAN INDIEN 2007–2013. We computed a slope map that we use to define the surface state and defined, accordingly, four different zones based on slope ($0\text{--}5^\circ$; $5\text{--}10^\circ$; $10\text{--}20^\circ$; $> 20^\circ$) (Fig. 3).

Rivers, channel, lakes represented in the different maps come from the 1/10 000 hydrogeography database of the FTM (Fig. 3). The land-cover database was obtained from the same institute. We used only three land occupation zones: rice-growing culture, swamp areas and lakes because they imply a near surface water-table, a key parameter relevant for geotechnical mapping and construction (Fig. 3).

The geological base map was obtained by digitizing the geological map (sheet PQ 47 Antananarivo – Manjakandriana, source: Ministry of Mines – Ampandrianomby) (Fig. 4).

2.3. Underground database

In the Antananarivo area, the Laboratoire National des Travaux Publics et du Bâtiment (LNTPB) has provided an access to the borehole data they collected from 2005 to the present day. We were thus able to build a database combining boreholes that have different origins. Most were linked to geotechnical investigations related to urban development and building construction, but the database also includes specialized geotechnical investigations including a slope stability and dimensioning study, and a study about compressible zones for earthwork. The dataset comprises 221 boreholes, which locations are displayed in Fig. 5. The lithological data (clay, slit, sand, peat) indicated in the logs were used to unravel the weathered subsurface structure of the Antananarivo area (Fig. 5).

In addition to lithological information, we got 153 sites where piezometric levels are available (Fig. 8). These piezometric levels are particularly important for a geotechnical evaluation regarding excavatability, road construction, underground work. According to Gruber and Rodrigues (1994), piezometric levels below 1m must be considered as inadequate (Table 2).

In-situ geotechnical data are available for 154 sites. In situ geotechnical measurements allow characterizing the mechanical characteristic of the regolith (Table 1), and comprise here pressuremeter test and dynamic penetration test measurements with measurements of limit pressure (PL)/pressuremeter modulus E/Advance dynamic Strength Qd (Fig. 6). The Limit Pressure PL corresponds to an applied pressure such that the material enters a plastic state and the deformation accelerates up to the complete failure point, the pressuremeter modulus E corresponds to an applied pressure such that the material deformation is recoverable (elastic behavior). These data were directly used in computing the soil bearing capacity (Appendix I) and in the resulting geotechnical mapping (see below).

In addition to in-situ geotechnical measurements, we got ~74 laboratory geotechnical measurements on borehole samples comprising cohesion, friction angle and bulk density, among others in the study area (Table 3). The data was also used to compute the soil bearing capacity (See Appendix).

2.4. Geotechnical mapping

As our aim is to help developing a sustainable urban planning, we seek to produce a geotechnical map combining geological, geomorphological and land-use maps with geotechnical parameters relevant for foundation building. The resulting cartographic products seek to facilitate the first stage of a safer urban development (e.g. El May et al., 2010). We present two GIS cartographic products.

We first applied a simple GIS methodology in the ARCGIS software in a way similar to Martínez-Graña et al. (2013) and many others (e.g. Dai et al., 2001; Aly et al., 2005; Berhane and Walraevens, 2013). We

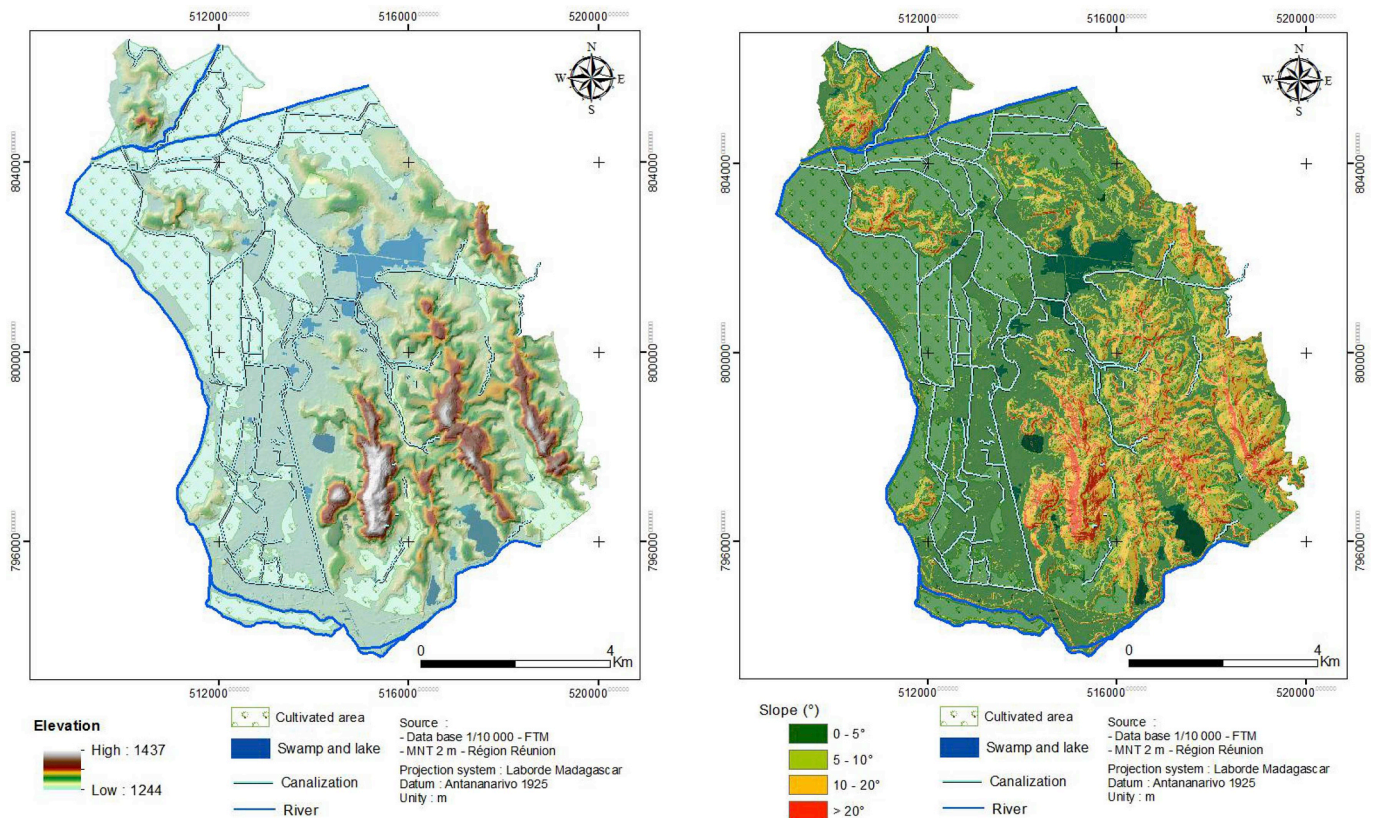


Fig. 3. Topographic (top) and slope map (bottom) using a 2m resolution MNT (Région réunion) with river network and land use according to database of FTM. The topographic map evidences three large ridges located mostly in the southeastern part of the study area. It comprises from west to east, the Rova Ridge, the Observatoire Ridge and the Ankatso Ridge.

combine three base maps: lithology as a geological indicator (Dearman, 1991, Fig. 4), slope as a geomorphological indicator (Fig. 3) and hydrogeology to take into account the influence of ground water (Fig. 8). For the geological base map, we kept 4 geological classes: alluvium, migmatitic granite, gneiss, migmatite. For the geomorphological base map, we defined 4 zones based on slope: 0–5°; 5–10°; 10–20°; > 20°, except for alluvium. Indeed alluvial deposits have generally a slope inferior to 5°. In the MNT with a 2 m resolution, higher slope values are due to human constructions (distinctly apparent linear structure on the MNT in Fig. 5). We thus have defined 13 units with different ground conditions based on the combined base maps. Regarding the hydrogeological parameters, the piezometric levels obtained in boreholes (Fig. 8) are represented following the classification scheme of Gruber and Rodrigues (1994) exposed in Table 2. Finally, this first cartographic product (Fig. 9) is associated with a table presenting the range of underground geotechnical values in the different units (Table 3).

Our second cartographic product (Fig. 10) uses the soil bearing capacity that is a geotechnical parameter integrating pressuremeter data and the laboratory measurement acquired for each borehole. We can obtain in that way a single meaningful geotechnical parameter for each borehole that is directly useful regarding urban construction. We computed the soil bearing capacity here considering foundations based on 1m square insulated footing with 50 cm long anchors (Gruber and Rodrigues, 1994), because it is relevant for most of the building in Antananarivo. We used the DTU 13.12 (1988) empirical rule because it is the one used in Madagascar and in French speaking countries (Arnould, 1974). For every boreholes with geotechnical data, the GEOFOND software was used for all computation. The appendix is indicating how the computation was done. The soil bearing capacity was obtained for 132 boreholes. The parameter was then interpolated by krigging. We tested different interpolation method with this very

irregular and inhomogeneous data set, and krigging provides the most relevant interpolation. The results are presented using the classification table of Hrasna and Vilcko (1994) (Table 4) in Fig. 10.

In the last cartographic product of the geotechnical data, hydrogeology was represented because it is a key parameter in any engineering geological map (Dearman, 1991). So the soil bearing capacity map was presented with the shallow > 1 m piezometric levels obtained in boreholes. The map was also combined with a very conservative estimate of areas with a shallow > 1 m water table based on land-cover data (lake, swamp and rice field) that are flooding prone. These areas are not suitable for construction purpose without extensive filling (see Table 2).

3. Results

3.1. Geomorphology

The city of Antananarivo is located in the central highland region of Madagascar. It is divided into three hill ranges rising 200m above a lower plain. The relief is inherited from tertiary and quaternary climatic conditions (Bourgeat and Ratsimbazafy, 1975), and generally comprises ridges, slopes, broad valleys and alluvial plains (Hoeblich and Hoeblich, 1983).

Ridges, hills and slopes form about 42% of the Antananarivo area, which represents about 36 km². Ridges are found in the southeastern part of the study area; they are organized in three main elongated and rounded ridges striking NNO – SSE (Fig. 3), that reach 1435 m a.s.l. (above sea level). The highest and western ridge is called the Rova Ridge, the central one, the Observatoire Ridge, and the eastern one, which bounds completely to the east the Antananarivo area, the Ankatso Ridge. Their slopes are divided in three levels: the upper one from

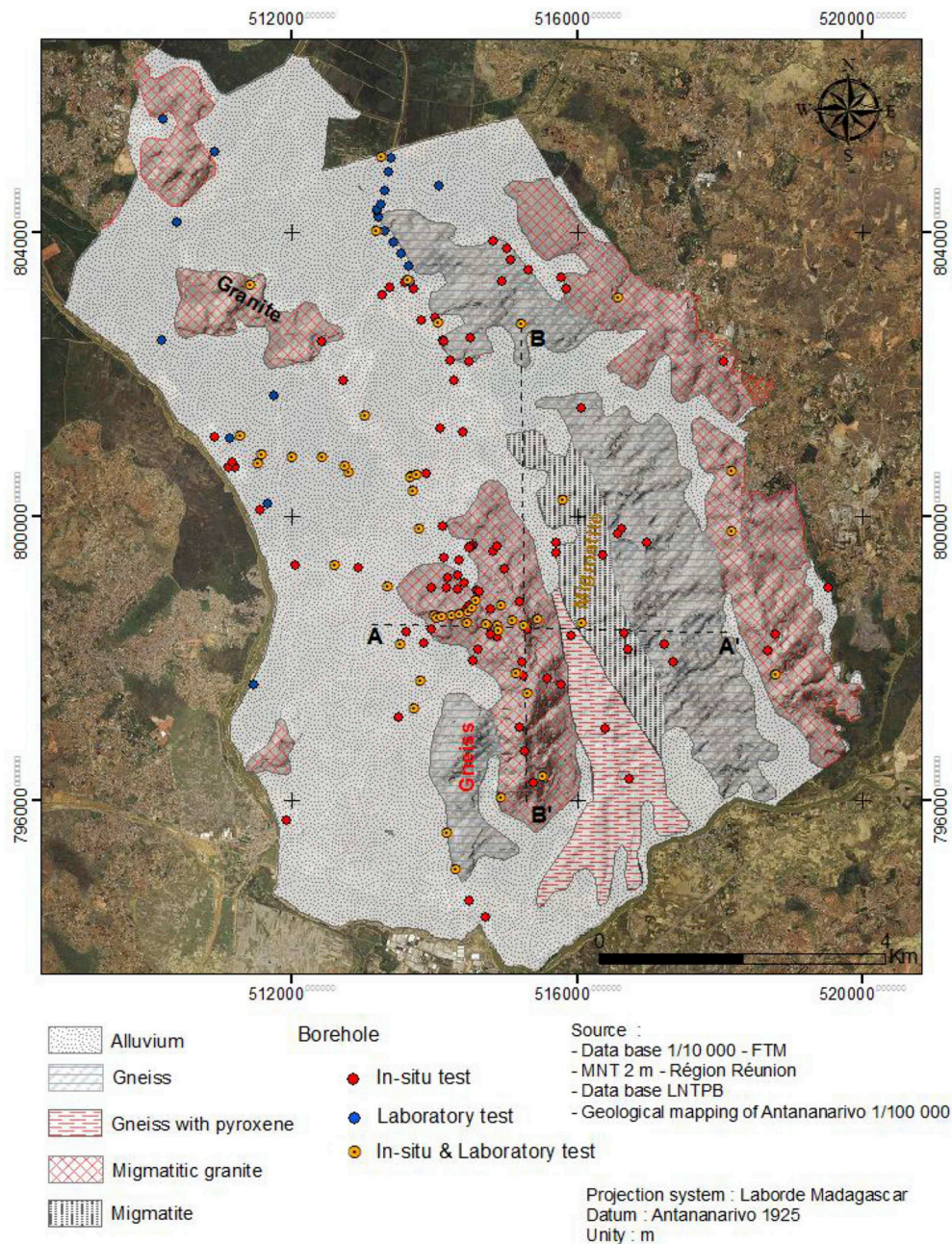


Fig. 4. Geology of the Antananarivo area and borehole used in the present study; Red: In-situ data, Blue: Laboratory data, Orange: In-situ & Laboratory data. Cross sections A-A' and B-B' in Fig. 5 are indicated with dash lines. (For interpretation of the references to colour in this figure legend, the reader is referred to the Web version of this article.)

1350 to 1360 m with high slopes reaching 40°, the intermediate one around the average altitude of 1300 m with slopes ranging from 2 to 70° and the lower one between 1265 à 1270 m with lower slopes mostly below 5° (Hydretude, 2015). The two upper levels are highly eroded by multiples gullies; the lower level is characterized by the deposition of colluvial material resulting from upslope erosion. Two lower hills are found to the southwest and southeast of the Rova Ridge. In the northern half of the study area, 3 others low hills stand above the plain. During very heavy rainfall associated with cyclones originating over the Indian Ocean, hillslopes are affected by landslides.

Valleys and alluvial plains cover 58% of the Antananarivo area, which represents about 50 km². Valleys stand parallel to the ridges and are wide convex area with very low slopes (Fig. 3). They are filled by alluvium and are occupied by lakes, wetlands, rice field and rivers as indicated in the land-cover data. The wide alluvial plains of the Ikopa

River, and its tributaries the Imamba and the Ankosy Rivers occupy the northern, western and southern part of Antananarivo area (Chaperon et al., 1993). The Ikopa floodplain has been drained and has historically been occupied by rice fields (Delubac et al., 1963).

3.2. Geology

Two type of formation are found, an old crystalline basement and an alluvial zone in the Antananarivo plain (Fig. 4). The basement comprises gneiss (> 2600 Ma), granites (~1000 Ma) and migmatites (550 Ma) (Delbos, 1960) and is intruded by the Ambatomiranty formation (not represented in Fig. 4). Gneiss terrains comprise gneiss with pyroxene and gneiss with biotite and sometimes amphibole or graphite. The first one has less the characteristic of a migmatite than the second one; it is more resistant to chemical weathering and spans 3.4 km². The

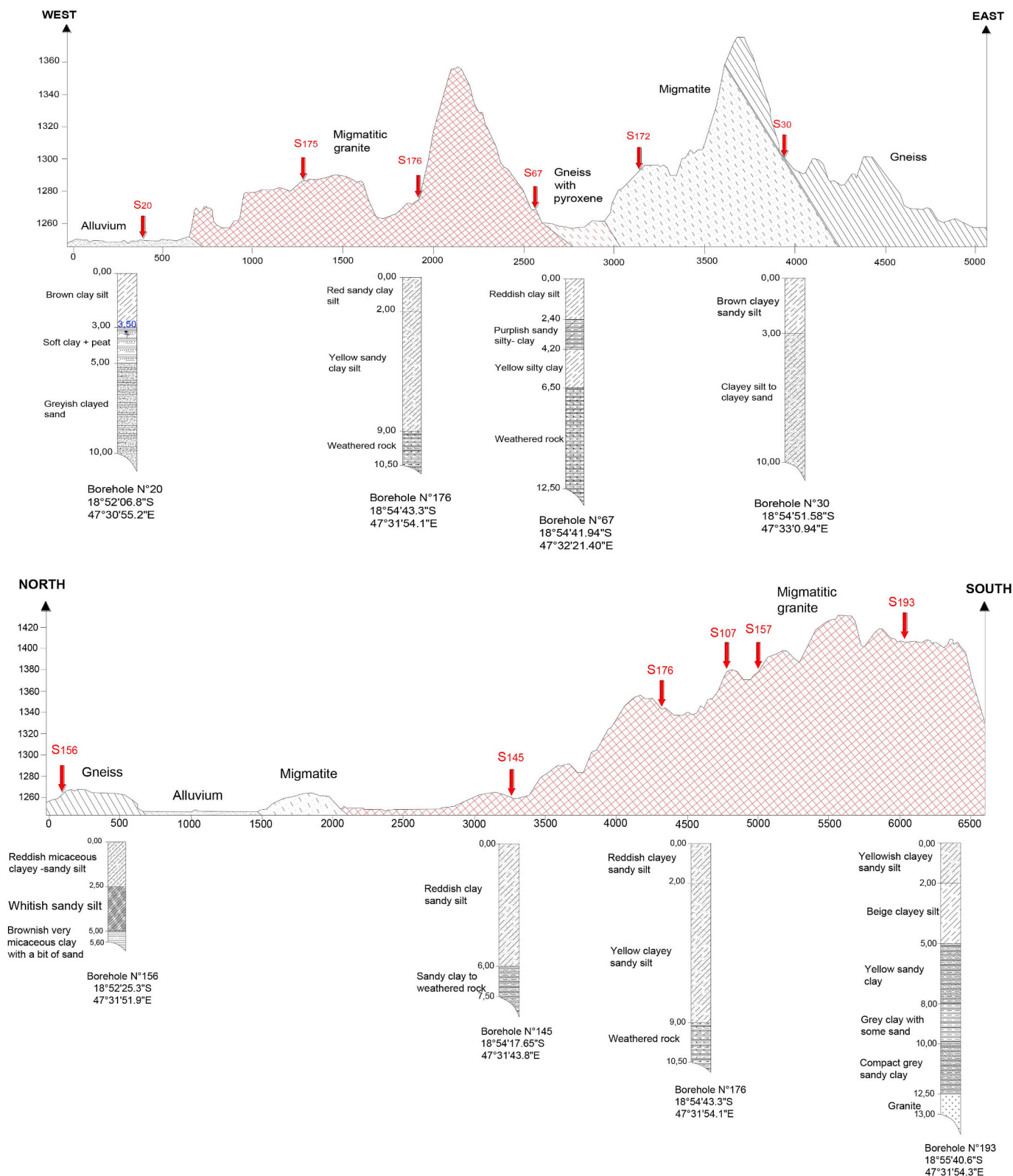


Fig. 5. Topographic section (see location in Fig. 4) and characteristic lithological logs of boreholes.

second one covers 14% of the study area. Granitic terrain comprises the granite of Ambatomiranty, migmatic granite and migmatite granitoid. Veins of the Ambatomiranty formation cross-cut the stratification with a SW-NE strike and are found in the southern part of the city. It shows the typical spheroidal weathering of granites. Given the large strength of this formation, it is often used for paving and in other constructions.

Migmatic granite and granitoid migmatite occupy more than 20% of the capital city. The two granites are typical of the central area of Madagascar and it is difficult to distinguish between them. The structure of these formations leads to poor mechanical performance, so they are used only as rubble stone in construction. Migmatite covers 3.6% of the study area (i.e., 3 km²) and are often associated with gneiss (Delubac,

Table 1

Geotechnical characteristics of regolith on top of the different basements with F %: Fine percentage ($< 80 \mu\text{m}$); LL: Liquid Limit; PL: Plasticity Limit; Sr: Degree of saturation (%); γ : Apparent volumetric weight (kN/m^3); c: Cohesion (kPa); φ : Friction angle ($^\circ$); e_o : Void index.

	Alluvium	Gneiss	Migmatite	Migmatitic Granite
%F	18 à 99	8 to 87	–	28 to 65
LL	25 to 306	20 to 72	–	28 to 60
PL	6 to 167	6 to 39	17	11 to 20
Sr	73 to 111.1	–	–	29 to 82
γ (kN/m^3)	10.6 to 20.4	14.8 to 18.9	15.3 to 19.3	14 to 19.6
c (kPa)	0 to 28	3 to 28	10 to 16	2 to 48
φ ($^\circ$)	0 to 32	21 to 35	7 to 30	4 to 40
e_o	0.608 to 8.073	2.085	–	0.630 to 1.239

1963). They show parallel continuous and weathered beds striking NE-SW (Ratsimbazafy, 1972) and represents less resistant areas like the gneiss terrains.

All hills and ridges are composed of this weathered crystalline basement (Fig. 4). The highest western Rova Ridge, the two low hills more to the northwest in the plain and the eastern Ankatso Ridge are made of migmatitic granites. The crest and the eastern hillslope of the central Observatoire Ridge are made of gneiss, and its western hillslope of migmatite. The two low hills located respectively, to the northwest of the Observatoire Ridge and to the southwest of the Rova Ridge are also made of gneiss. The last low hill to the southeast of the Rova Ridge is made of gneiss with pyroxene and Anbatomianty granite.

The Quaternary alluvium deposited in flat plains of the Antananarivo area comprised lacustrine, alluvial, colluvial and swamp deposits. It covers 58% of the study area. The alluvium comprises clay, silt, sand and peat layers.

3.3. Urban characteristics of Antananarivo

Urbanization spreads beyond the city's official boundaries (Fig. 1C), and the whole urban municipality may reach ~ 6 millions in 2030. However the present study is limited to the official boundary of the capital. The capital is divided in 6 boroughs and 192 village districts (called Fokontany) having 700 to 26 550 inhabitants (Fig. 1C). The urbanized area has a mean density of 250 people/ha, but a high density of 700 people/ha can be reached (Rajaonary and Rafanoharantsoa, 2012).

Maps showing the density of population (Fig. 1C) and the density of building and road system (Fig. 1D) show a very heterogeneous city. This heterogeneity was initially linked to the local geomorphology with a more extensive human occupation (population and construction) of the hills and ridges rising 200m above a lower plain and agricultural fields in the lowland. Indeed historical construction are located on ridges where they are protected from flooding, the highest risk in Antananarivo, whereas the best places for agricultural fields and particularly rice field are in the flat plains are regularly inundated during cyclonic periods (Fig. 3). The occupation of the hills is still strongly heterogeneous (Fig. 1). It is linked to the historical occupation of mainly the western most Rova Hill located the closest to the main Ikopa River and the agricultural fields (Figs. 1 and 3). Most of the political power and administration is still centered on or near the Rova Ridge, and the road network displays a dense radial pattern on and around it. The main node of the road network is located on the northern end of this ridge, near the central railway station. This historical district has a homogeneous high density of population and building, and a good network of roads. The two lower hills just to the southwest and southeast also have a high density of population and building associated with a significant road network. More to the east, the Observatoire Ridge is also populated, but its density in population and building are greatly influenced by the road network that is not as well

developed as on the Rova Ridge. The building density seems a direct function of the proximity of the main road system. Along the eastern edge of the Capital area, the Ankatso Ridge is very poorly deserved; the building and population density are very low compared to the two other ridges, and directly dependent on the main road network. On the opposite, in the northern half of the Antananarivo area, the three low hills standing slightly above the flat flooding prone plain are well deserved and show a relatively high population and building density.

Since 1960, the flat plain have started to be occupied in parallel with the development of flood protections, filling and embankments (Rajaonary and Rafanoharantsoa, 2012; Rambinintsoa, 2012). Agricultural lands were progressively replaced by recent residential and commercial buildings (Rajaonary and Rafanoharantsoa, 2012; Rambinintsoa, 2012). Despite its dewatering by an extensive drainage system (Fig. 3), flooding occurs regularly during cyclonic periods.

Settlements in these flat areas were needed to accommodate a large urban migration (Razafimanjato et al., 2001). In addition, constructions in these flat areas were easier and cheaper to build than on the crowded Rova ridge that was lacking cheap plots, easily buildable and accessible areas. However the urban development in these flat terrains was anarchic and did not follow any precise urban management plan. The urban hotspots there stand close to the historical, economic and administrative center on the Rova Ridge. A large one developed just in the wide alluvial plain west of the Rova Ridge, and another one in the narrower valley northeast of the Rova Ridge and east of the Observatoire Ridge (Figs. 1 and 3).

3.4. Hydrogeology and flooding

The mean piezometric levels in boreholes vary from 0.60 to 6.75 m, and show a simple link with topography (Figs. 3 and 5). On the ridges near the crest, there is no underground water stored and at slightly lower elevation and on slopes, the ground water level is usually deeper than 1m and can reach 5m.

In the flat plain, the situation is different. The piezometric levels are fluctuating: ground water is very shallow ($< 1\text{m}$) during the rainy season, and can fall significantly at the end of the dry season (Artelia, 2014). The groundwater level can also be influence by the presence of thick clay layers that form an aquiclude and that are favoring a shallow water level and flooding. The water table level can thus be heterogeneous in the flat plain, which what is shown in the borehole data (Fig. 8). In the central lowland, northwest of the Rova Ridge most borehole data indicates a very shallow water level. In the lowland between the granitic Rova Ridge and the granitic hill to the north-northeast of the Rova Ridge, boreholes indicate a deeper water table (1–5 m). Similarly some boreholes west of the Rova Ridge indicates a deeper aquifer, but our data density is too low to be conclusive.

To complete the record of piezometric levels, we use specific land-cover categories (rice-field, lake, swamp areas) that indicate shallow ground water (Fig. 3). The largest swamps/lakes are concentrated north and south of the Observatoire Ridge, and west of the low gneiss hill located northnorthwest of the Observatoire Ridge. They are systematically associated with gneiss and migmatite terrains, which weathering can produce thick clay layers. The rice fields are mostly located close to the main river system, but in the north some are close to the lake/swamp areas.

A first crude evaluation of the flood prone areas thus comprise these land-cover categories and the borehole location with a $> 1\text{m}$ water table. Any constructions there would require an extensive use of embankments and infilling, which is extremely common in Antananarivo. However any urban development in flood prone area would lead to even more severe flooding due to water flow constriction as observed by Rambinintsoanintsoa (2012). In addition, because of the extensive use of embankments and infilling of poor quality, these low areas are now prone to landsliding in the compressible soils of embankments.

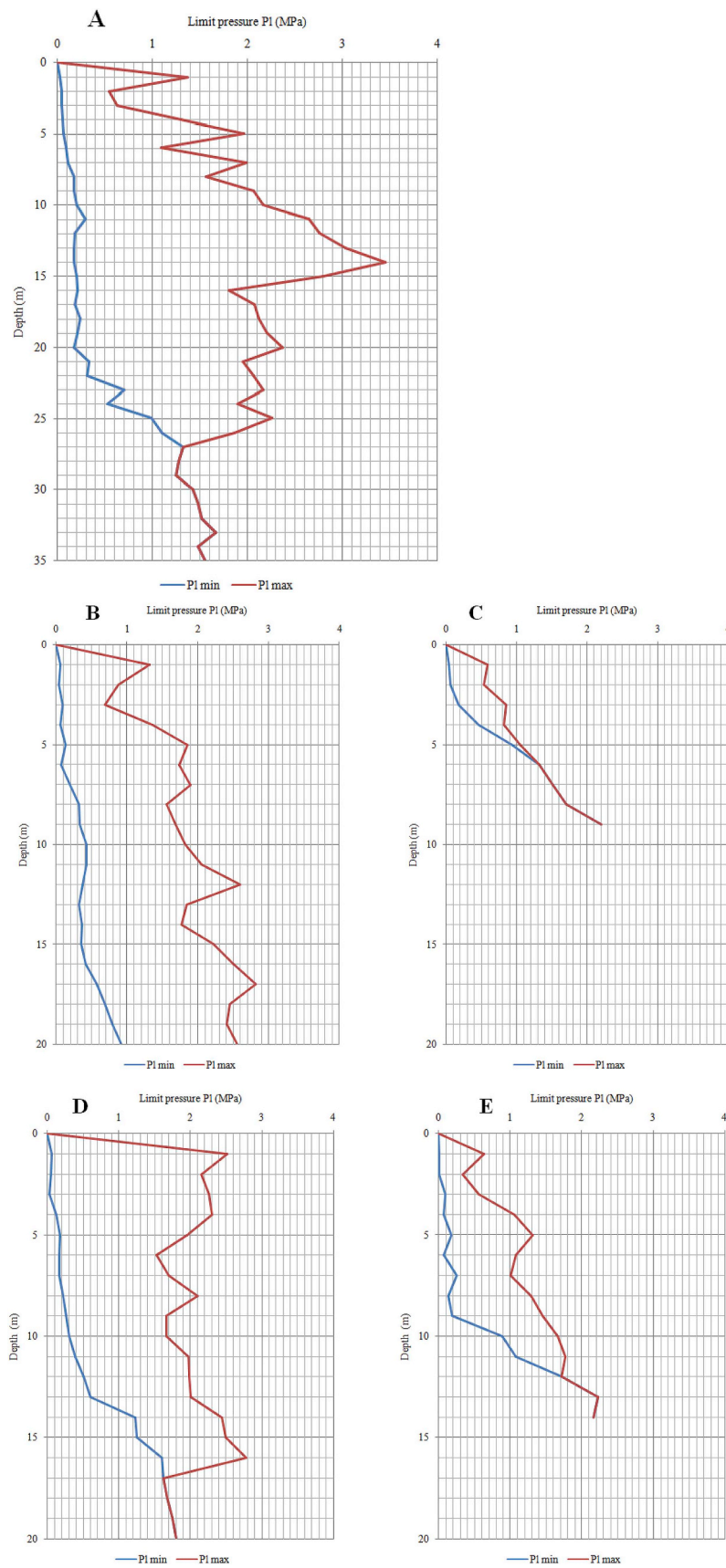


Fig. 6. Minimal and maximal limit pressure measured in the regolith cover above the different geological basements in the study area. A: Alluvium, B: Gneiss, C: Pyroxen Gneiss, D: Migmatite Granit, E: Migmatite.

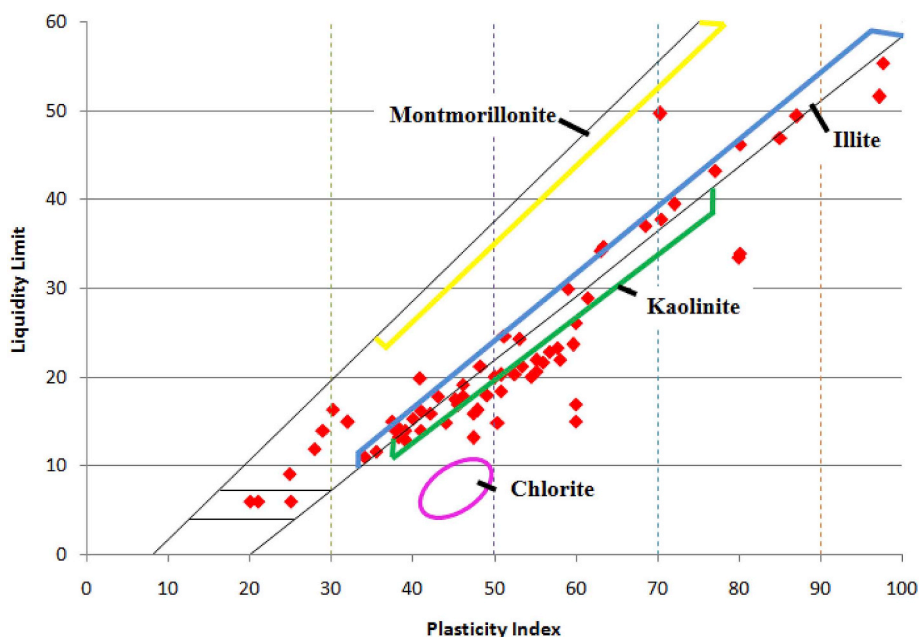


Fig. 7. A plasticity chart showing with typical behavior of clay minerals (montmorillonite, kaolinite, illite, chlorite). Samples from the Antananarivo urban community are plotted with red diamonds. (For interpretation of the references to colour in this figure legend, the reader is referred to the Web version of this article.)

3.5. Subsurface characteristics

Selected samples of the boreholes are represented in two north-south and east-west cross sections with their lithology (Fig. 5). In the following, we distinguish here the quaternary alluvial area occupying the flat areas from the ridge, because sediments in the former are provided by river network whereas the latter results from in-situ chemical weathering. Limit pressure data are presented in Fig. 6 because they are key parameters in dimensioning for suitable foundation that we will use for building geotechnical map.

In general, in the alluvial plain, the underground is very heterogeneous with alternation of clay, peat and sand layers. It is generally composed of a top alluvial part rich in clay and silt, and a bottom part that can be more sandy resulting from in-situ weathering (see S-20, 191 et 124 display in Figs. 1, Figs. 5 and 6). Alluvium thickness varies significantly. Around Ankorondrano (S219, Fig. 1) in the NW part of Antananarivo, alluvium can reach 15.50–32.50 m and in the district of Antohata penaka, in the “village de la francophonie (see location in Fig. 1), it reaches 35m. The series and mix of clay, sand, silt and peat layers composing the alluvial sediments have the following characteristics. Clays are prevalent in river bed and swamp areas, and can reach 10 m like in Ankorondrano, Tsaralalana, Analakely areas (Fig. 1). They are often associated to silt and sand, but are different from deeper clays associated with silt and sand that results from the weathering of the crystalline basement. Sand layers are mostly siliceous, but can be micaceous and can reach thicknesses of 15–27 m like in Village Voara, Andohatpenaka, HJRA Ampefiloha, Ankorondrano (see locations in Fig. 1). Peat layers are often associated with clay layers, they are often irregular and discontinuous, but can reach a thickness of 5 m (in borehole for the eastern bypass project).

Alluvium in the flat plain and valleys have specific geotechnical properties with a void index that can be very high (Fig. 6 a). For the alluvium (A), the low deformation limit pressure values in near top layers correspond to swampy zones or low compactness embanked terrains. They are soft soils (peat and clay) considering that the pressure limit can inferior to 0.70 MPa (Vulliet et al., 2016). These clay layers in the alluvium can have a very high plasticity and liquid limits. The basal sand-richer unit is strongly strengthening downward with increasing compaction.

Regarding the crystalline basement, it is covered by a typical loose regolith layer with a top ferrallitic soil (Ramifehiarivo et al., 2016) resulting from tropical weathering (Gutiérrez M., 2013). The different basement geology results in a difference of regolith thickness (Fig. 5). Gneiss and granites have been subjected to a deep chemical weathering that has transformed all feldspar in kaolinite and gibbsite. The weathering of mica, and of K-feldspar could lead to the formation of illite. On hills, the resulting regolith can reach a thickness 15 m depending on the drill location, the local geomorphology (ridge, slope, low concave area favoring infiltration versus runoff) and the form or aspect of the substratum. The boreholes on the crystalline basement show a regolith cover with a 12 m average thickness composed of a succession of mostly clayey silt to silty clay layers in the top half top, sandy clay to clayey sand in the bottom half. Boreholes show large variations in regolith thickness. Around Andohalo, bedrock outcrops at (Lapan'nyTovolahy, Fig. 1), but is found at 10.50 m depth in S107 (lycée Maria Manjaka); around the Fokontany of Ambohimitsimbina (S193), unweathered rocks are found at 13.00 m depth, and at ~5 m depth further south (S220)(Figs. 5 and 6).

In-situ geotechnical measurements allow characterizing a mechanical characteristic of the in situ weathered top cover. The typical profiles of the minimum and maximum Limit Pressure PL for the regolith cover above the different geological basements are displayed in Fig. 5. Generally, in all profiles, there is strengthening with depth due to compacting under due the weight of sediments above like for the borehole in the alluvium. For the first depth meters, and even more, the large limit pressure may also be related to compaction induced by vehicular traffic and construction. The thickness of the regolith cover over the basement is also an important factor, in particular for profiles sampling the same geological unit. In fact, for the granitic hill (D), the basement is situated at less than 1 m depth, the in-situ measures carried out give a limit pressure greater than 2, which is not the case in other sites with the same geological basement but with a thicker lateritic cover.

The data show that granite has the strongest average compressive strength at depth of 61 MPa and a volume weight of 25.2 kN/m³ (e.g. borehole S220). In the migmatite zone (e.g. borehole S81), the rock average compressive strength is 43 MPa and a volume weight of 26 kN/m³. Geotechnical characteristics of the regoliths above the crystalline

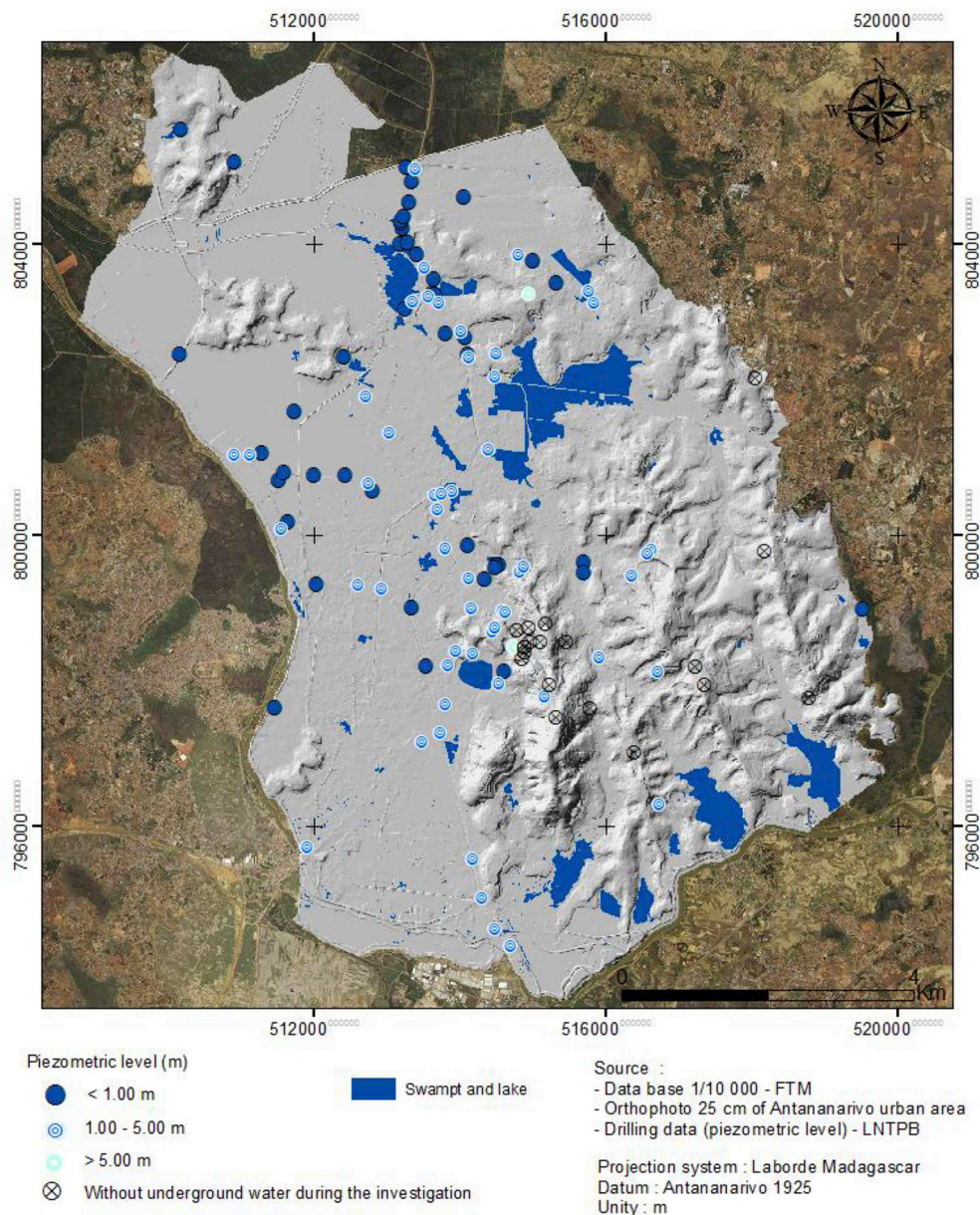


Fig. 8. Piezometric level measurements and topographic representation of the urban area of Antananarivo.

Table 2
Suitability classes depending on ground water level for different excavations (Gruber and Rodrigues, 1994).

	Adequate	Reasonable	Inadequate
Excavability chart	> 5m	1–5 m	< 1m
Underground work chart	> 5m	1–5 m	< 1m
Road construction chart	> 1m		< 1m

basement are listed in Table 1. Strongest regolith lies on top of the granite magmatic basement; it displays a relatively low plastic limit < 20, void index < 1.25; cohesion and friction can reach high values. Regolith on gneiss is weaker. In addition, near the slope base, less resistance thick clay layers can be found, the discontinuity formed by the junction on the regolith and the substratum may be related to former landslide episodes.






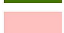



Two laboratory geotechnical measurements, the liquidity limit and plasticity index provide further information. These indexes depend on the grain-size and type of clay present at depth. Well-established

empirical methods based on the Atterberg limits can be used to reflect the swell behavior of a clay soils (Holtz and Kovacs, 1981). Fig. 7 represents the Atterberg limits obtained from the laboratory geotechnical measurements of 80 samples from the city and its periphery. The plasticity chart, which contains the ranges for montmorillonite, illite, kaolinite, and chlorite clays, shows that clay types are illite and kaolinite.

Kaolinite is a 1:1 type clay mineral, composed of one tetrahedral sheet (SiO₄) linked to an octahedral sheet (Al₂O₆); it has low swelling behavior due to the bonding of oxygen and hydrogen between the sheets (i.e. Vulliet et al., 2016). Illite, which is a typical weathering product of low grade metamorphic rocks, is a 2:1 type clay minerals, composed of an octahedral sheet between two tetrahedral sheets, and a Si/Al ratio of 2. Illite is nonexpanding clays due to the presence of K (or sometime Ca and Mg) interlayer cations which prevent the intrusion of water molecules into the clay structure; little water can be stored in between the clay sheets like for kaolinite. The behaviors of illite and kaolinite are quite similar, they store small quantity of water, and their low porosity reduces infiltration and increases run-off. The main

Table 3

Explanation table with legend of Fig. 9 and geotechnical characteristic of the units, with %F: fine percentage (< 80 µm); LL: Liquidity limit; Pl: Plasticity index; g: Apparent voluminal weight (kN/m³); c: cohesion (kPa); φ: friction angle (°).

Formation	Unit	Caption	Water table	%F	LL	Pl	g	c	φ (°)
Alluvium	a _I		Depth of the water table is between 0.10 and 4 m with average of 1.23m that could be qualified as reasonable for the realization of the excavation	18 to 99	25 to 306	6 to 167	10.6 to 20.4	0 to 28	0 to 32
Gneiss	G _I		Water table average depth is 3.47m, reasonable for the excavation	87	72	39	14.8	3	2
	G _{II}		Water table average depth is 1.51m and is suitable for the excavation	–	–	–	16.9	28	12
	G _{III}		No ground water is detected during the investigation	8 to 68	20 to 52	6 to 20	15.4 to 18.9	3 to 19	29 to 35
	G _{IV}		No ground water is detected during the investigation	–	–	–	18.9	3	35
Migmatitic Granite	MU _I		Water table average depth is 2.48m. It is reasonable for the excavation.	39 to 59	28 to 51	12 to 20	14.9 to 17.25	10 to 38	4 to 21
	MU _{II}		The water table average depth is 4m. It is reasonable for the excavation	28 to 58	29 to 60	11 to 15	14.3 to 18.8	2 to 48	8 to 27
	MU _{III}		No ground water is detected during the investigation	38 to 64	32	12 to 15	16.5 to 19.6	4 to 29	8 to 31
	MU _{IV}		No ground water is detected during the investigation	34 to 65	32 to 50	11 to 20	14 to 18.7	3 to 29	12 to 40

difference between illite and kaolinite is related to their different cation-exchange capacity (CEC), which affects infiltration. Cation exchange capacity (CEC) is one of the important properties in clay minerals. CEC is a measure of the capacity of clay minerals to exchange cations from the solution, which depends on the magnitude of the total layer charge. The cation-exchange capacity (CEC) of illite (10–40 meq/100g) is higher than that of kaolinite, typically around 3–15 meq/100 g. It indicates the illite capacity to retain cations and then to absorb water at the sheet surfaces is larger than for kaolinite (Murray, 2007), i.e. the negative area of the polar water molecules are attracted by the positive charge in the cations present in large quantity in illites. So the infiltration processes are generally reduced with illite compared to kaolinite.

3.6. Geotechnical mapping based on geological/geomorphological basemaps and soil bearing capacity

A secure urban expansion depends on the available knowledge of the subsurface characteristics, which would allow identifying any potential area unsafe for construction. Our first cartographic product (Fig. 9) is based on the data relevant regarding the subsurface state in a region like Antananarivo, for which we have an adequate continuous coverage: lithology and geology. They were used to defined 13 units with different ground conditions (Fig. 9), and the geotechnical data are presented in an associated expanded table displaying the range of geotechnical parameters of the different units (Table 3).

The geotechnical map (UNESCO, 1976) and associated table with the range of geotechnical properties (Fig. 9 and Table 3) have the following distinctive characteristics. Each class shows high values of the liquid limit (WL) and of the plasticity index (IP), which correspond to compressible and argillaceous layers with high content of water (Fig. 7, see supplemental material). These clayey rich layers are present in all boreholes (Fig. 5). These formations with a low porosity and water storage capacity have a larger thickness in low slope deposits and in the alluvial plain. They are favorable to water stagnation and lead to the formation of swamp areas and zones favorable to rice cultivations. The plasticity index (IP) values inferior to 12 correspond to less plastic soils composed of sandy units that are systematically present in all profiles even in the alluvial plain. The apparent volumetric weight values that range from 10.6 to 20.4 correspond to a presence of an extremely bad quality soil to an average soil according to the qualification table of Vulliet and al. (2016). Regarding shearing test, which are important for the stability and the design of foundation calculation, the cohesion and the internal friction angle are two key parameters. They constrain the material shear strength and are dependent directly on the lithology:

sand layers have low to no cohesion, but sand layers have larger friction angle and peat layers the lower one. These two parameters show a large spatial variability. In addition, they were measured under the laboratory condition, and cohesion is quite sensible to water pore pressure and changes in the water table, it is thus temporally variable.

The geotechnical cartographic product obtained in Fig. 9 and in the associated Table 3 that seeks to facilitate a safer urbanization is not fully adequate. This type of geotechnical mapping is limited in tropical areas compared to European countries where it has previously been used. Indeed each unit defined according to geological and geomorphological parameters shows a wide range of geotechnical properties (Table 3), weakly typical, which often overlaps with the geotechnical properties of other units. This is normal given the large change in geotechnical properties with depth at each borehole due to the deep chemical weathering (Figs. 5 and 6). That is why we choose to compute the soil bearing capacity for each borehole, which is a way to aggregated vertically all geotechnical parameters measured in a given borehole. In addition, the computed soil bearing capacity is a parameter that can be more directly use for urban planning purpose. This is particularly true in Madagascar, where most building have similar characteristics and thus similar geotechnical building requirement.

Our second geotechnical map is thus a direct visualization of the soil bearing capacity computed for each borehole and interpolated. We also include relevant information regarding the water table. Known low ground water level, land-use classes indicating shallow water level are indicated, because these area are inadequate for construction (Table 2) and we seek a complete cartographic product useful for planning urban constructions.

The resulting map in Fig. 10 shows three units. The unit in green is considered non suitable to the construction and comprises the areas with low bearing capacity (< 50 kPa), land use category indicating a < 1m water table thus not suitable for construction (swamp, lake and rice field); it corresponds mostly to low lying alluvial areas. They cover more than 40% of the urban area. This part of area is in influencing by water stagnation, shallow water table, variation of the water table depth, low degree of compaction of the superficial layer, clay with a high plasticity and high liquid limit. All of those conditions influence the mechanical comportment of soil. This is why this part of the city cannot is considering as not suitable for construction. The moderately suitable zone with a bearing capacity between 50 kPa and 150 kPa covers more than 55% of the city. It corresponds to most of the basement hills of the urban area. In hills, the soil mechanical characteristics and the influences of the low depth of the substratum justify the values of the bearing capacity of soil. The moderately suitable zone with 150–350 kPa bearing capacity covers less than 1% of the area study.

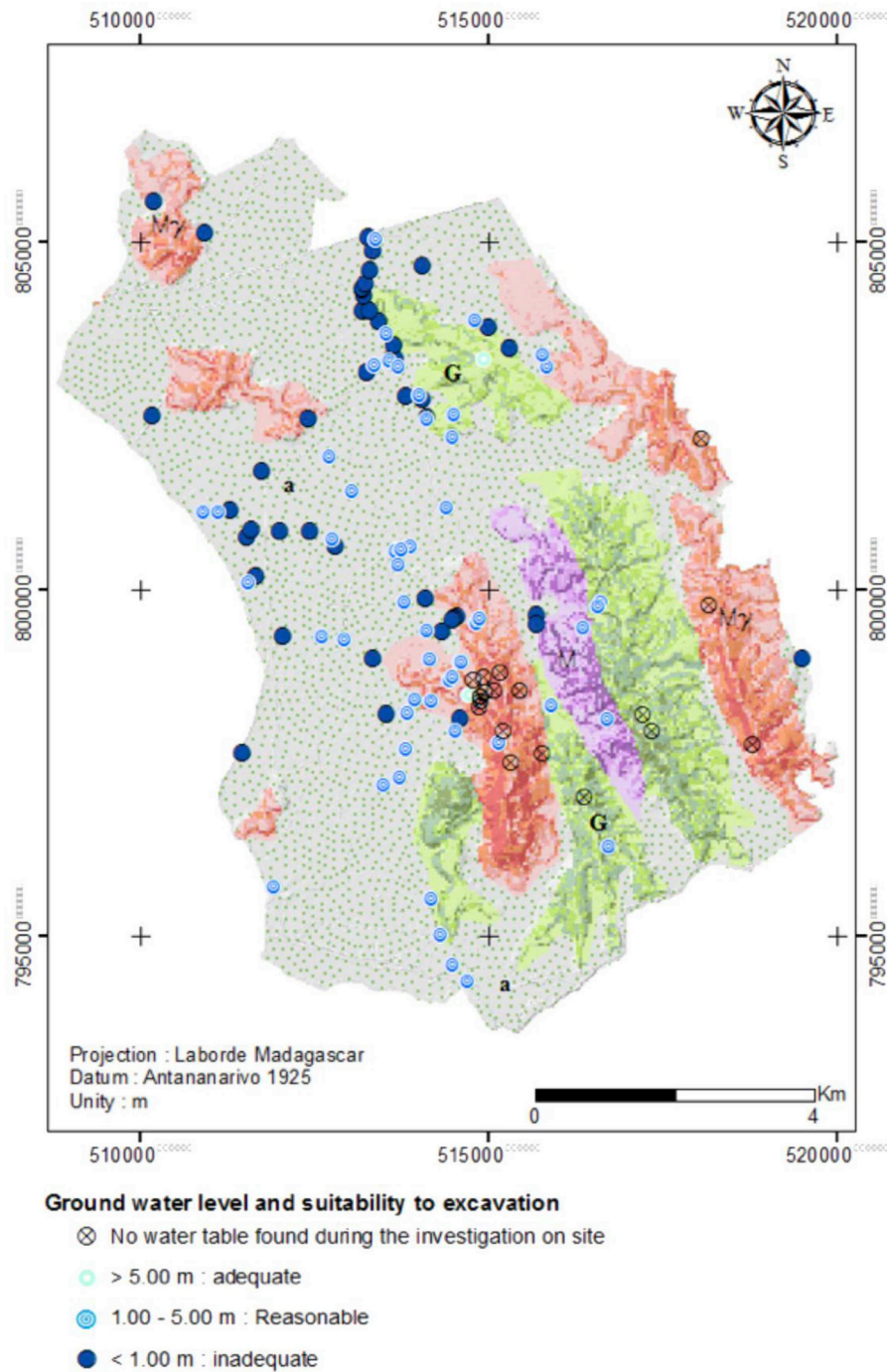


Fig. 9. Geotechnical mapping taking into account geological units (alluvium, migmatitic granite, gneiss, migmatite) and slope map (4 classes: 0–5°; 5–10°; 10–20°; > 20°) with the geotechnical characteristics of alluvium and regolith given in Table 3. The explanation table and legend of the units is given in Table 3.

The latter part is situated in the western part of the city of Ambatobe section (cf. Fig. 10). This result is probably due to the characteristic of the regolith in the hill and the lower depth of substratum rock included in the calculation of bearing capacity.

The second cartographic product obtained is more adequate than the first one, but is based on a very unevenly distributed geotechnical data set. So the interpolated results that are on display must be used with caution. It is a map that needs to evolve with time and with the addition of new geotechnical data related to new construction projects. A more uniform sampling of the Antananarivo area is needed. We thus consider that currently the two types of geotechnical maps with the associated table (Figs. 9 and 10 and Table 3) are complementary and that they must be used jointly for any urban planning.

4. Discussion

The fundamental target of a geotechnical map is a cartographic product that comprises all the relevant information to guide the territory system (Peter, 1969). Presently in all countries, a central problem is how to tackle an ongoing growing urbanization; urban geological mapping producing engineering geological maps and suitability maps for construction (El May et al., 2010) can contribute to a more sustainable urban development in Africa (Cobbinah et al., 2015; Culshaw and Price, 2011; Richards, 2009). The very fast rate of urbanization in Africa (UNDESA/PD, 2012) is particularly challenging and has been associated with an increase in urban poverty (Cobbinah et al., 2015). In the urban Antananarivo area, a first step of a safe urban expansion

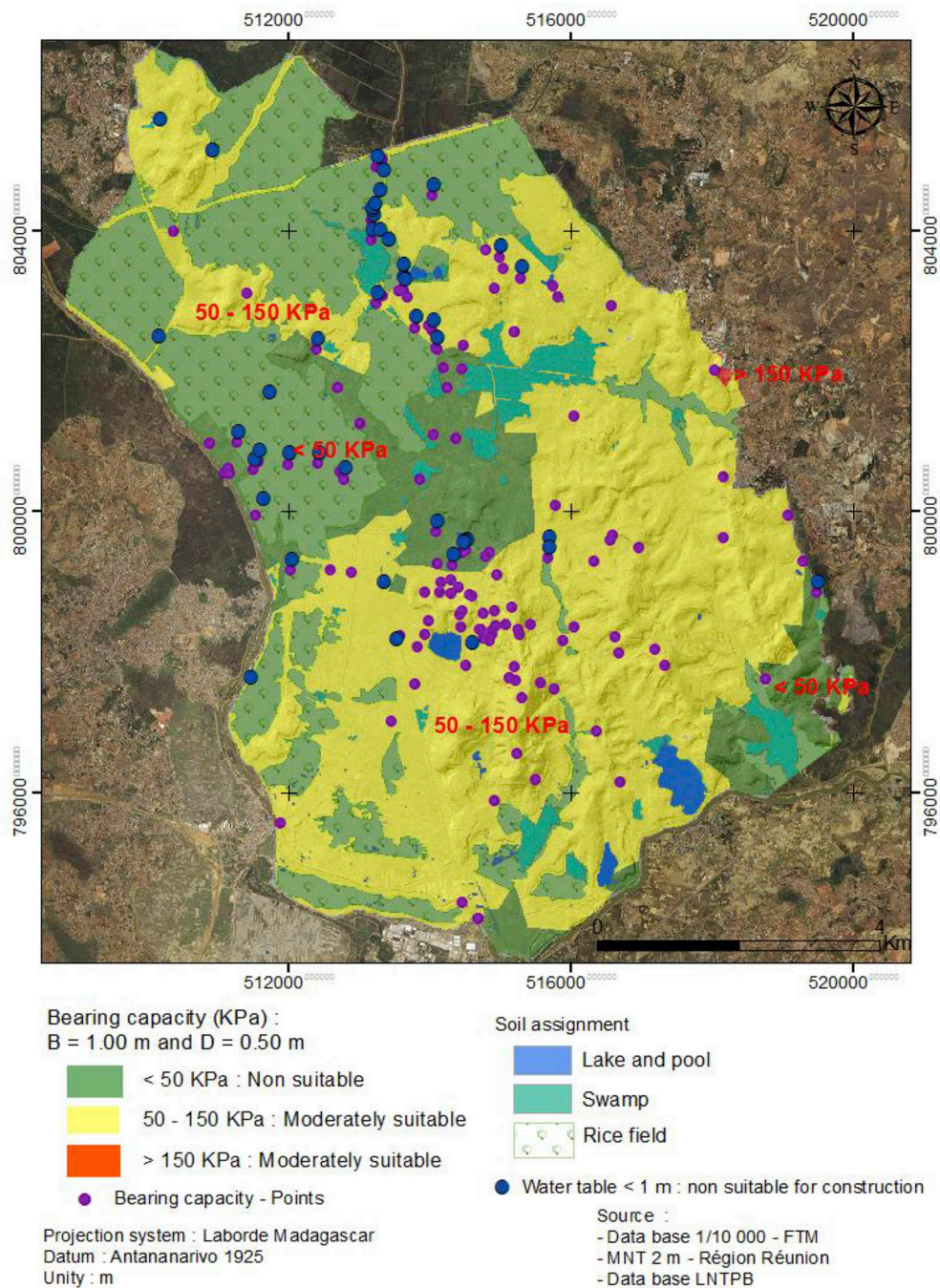


Fig. 10. Geotechnical mapping of soil bearing capacity obtained from geotechnical measurements (see appendix for the computation) and suitability to construction also considering land-use and piezometric levels.

Table 4
 Land suitability classes for construction depending on soilbearing capacity (Hrasna&Vilcko, 1994).

	Land suitability classes			
	Suitable	Moderatelysuitable	150–50	Non-suitable
Bearing capacity (kPa)	> 350	350–150	150–50	< 50

would be to build reliable foundations using geotechnical subsurface data. The presented geotechnical maps seek to provide relevant data to minimize the costly risk of unstable foundations. The problem of building collapse in Antananarivo in similar to the ones documented in

the largest city of Lagos (Davis, 2015) that was partly attributed to an inadequate understanding of the nature of the ground below constructed building (e.g. Una et al., 2015; Oyediran et al., 2015; Olatinsu et al., 2018). Building collapse is particularly crucial in country like Madagascar that has little resources for developing its infrastructures. The information provided by the geotechnical maps could thus be immediately used (1) to lower the feasibility cost at the beginning of any building project study, (2) to specify the technical prescription (i.e. the type of foundation, the level of the anchorage knowing the charges of the project), (3) to evaluate the adequacy between the project size and the chosen site. Urban planning is thus simplified and less costly.

Geotechnical maps could also reduce the number of the drilling or the sampling within a construction project, if there are already

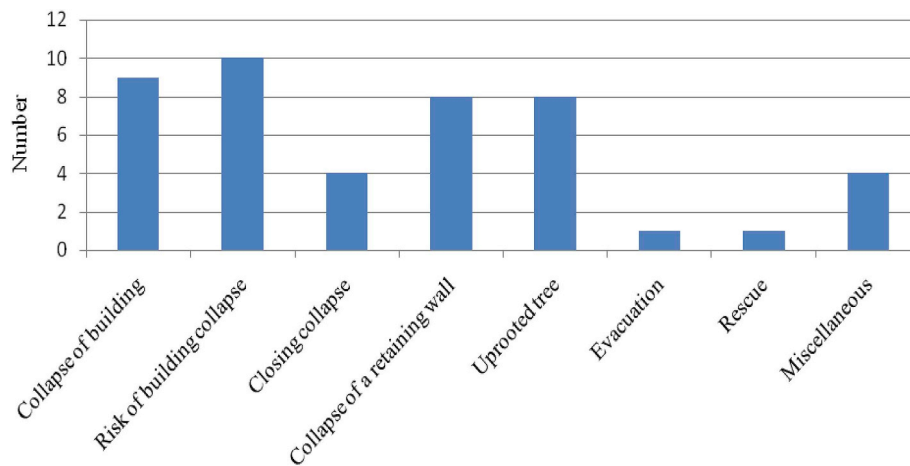


Fig. 11. Building demolition at risk of collapse in Antananarivo. Top: fire fighter operations statistics for January 2018 - (Source: Fire fighters). Bottom: A. Differential settlement of an R + 3 house foundation in Anjanahary II district O - 30th December 2017. B: Demolition of this house by firefighters to avoid collapse on surrounding environment (beginning of the year).

geotechnical data points in the same geomorphological and geological zone (Kadhim and Ahmed, 2015). It cannot however replace geotechnical investigation and drilling that need to take place before any building construction. The maps highlight the large spatial variability of the subsurface properties, and whatever the map precision and pre-existing boreholes, additional drilling will be needed to reduce the underground uncertainties for the safety of the project and to check the precision of the geotechnical maps. Future drilling, added to the present geodatabase, would improve the knowledge and value of the urban geology of Antananarivo.

Presently the geotechnical map is based on the soil bearing capacity (Fig. 10). It is a quantitative parameter used by builders that was also successfully used by El May et al. (2010) for the Tunis city. The map is built by interpolation of existing bear capacity data points, and its validity decreases sharply away from the drilling points. Our data base is not homogeneous in space and is unevenly distributed. The best coverage is on the western Rova hill made of migmatitic granites. At that location, we have the necessary sampling to have a representative and accurate geotechnical map. This mapping is particularly relevant, because the Rova hill has the largest population, the highest building and road density (Fig. 1). Even if the geotechnical parameters on most of the Rova hill indicate a location adequate for building, foundation degradation can still occur. This is the case of the Andafy Avaratra building near the palace of the prime minister that sustained

differential settlement due to water pipe leakage that saturated and softened the regolith cover (Appendix III-Fig. 1). Other hills have a weak coverage, and the reliability and the usefulness of the geotechnical maps at these locations will increase with time, when more boreholes will be added to the database. Regarding the alluvial plain, our map is also relevant in a context of the ongoing urbanization on these former agricultural fields that provided a reasonable number of geotechnical data used here. Our study emphasizes the rationale of building on the basement ridges and not in the alluvial plain.

Our geotechnical mapping and the associated recommendations face a difficult implementation given the situation on the ground. First, there is no precise urban planning, second there is no control by the responsible public authority on urban expansion, and third corruption is endemic. As a result many constructions are made without taking into account any environmental variable. About 70–80% of the building were constructed without a building permit and are thus illegal. So they do not comply with any building regulation. Constructions are made accordingly to the capacity of the designer at the lowest cost with a lack of control by qualified technicians. The most common problems are bad workmanship, latent defects, the improper sizing of the structure and sanitation issue due to construction errors in the foundation that can trigger water leakage. The lack of building maintenance and aging building are aggravating factors. As a result building damage and collapse are very common in the city of Antananarivo. Fig. 11 shows that

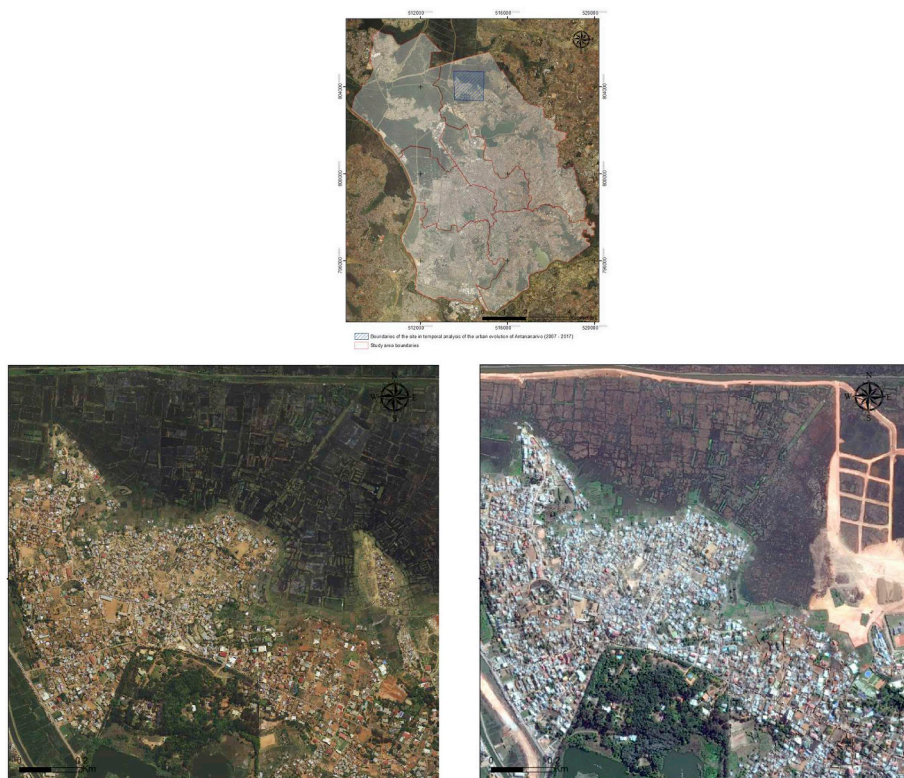


Fig. 12. Evolution of urbanization in the north part of Antananarivo from 2007 to 2017. Location of the Google images indicated by a blue frame in the top inset. (For interpretation of the references to colour in this figure legend, the reader is referred to the Web version of this article.)

in January 2018, a large fraction of the firefighter intervention was linked to building collapse (9 cases) and to the destruction of building at risk of collapse (10 cases). A similar situation has been documented in other large African cities including in Yaoundé and Douala in Cameroon (Tchamba and Bikoko, 2015). Building collapse are particularly frequent and well studied in Nigeria in the city of Lagos (Dimuna, 2010; Ede, 2013; Davies, 2015), and their origin are due to a number of reasons (Oloyede et al., 2010) including building materials (Amadi et al., 2012), subsurface conditions (Oyediran and Famakinwa, 2015), and incompetent builders (Dimuna, 2010). For the Antananarivo area, the problem is further magnified because it is located near a tropical cyclone belt, a situation that Asian cities also face (Gupta and Ahmad, 1999).

In addition, the city of Antananarivo is rapidly growing as illustrated in Fig. 12 showing the evolution of its northern part between 2007 and 2017. Already in the 90's the city and its suburbs were growing at a rate of about 4% per year, and at that time most houses were classified as low standing lacking modern infrastructures (Banque mondiale, 1990). The present situation is worse, for two reasons. First, informal settlements (e.g. slums) are increasing, and building standards are decreasing. Second, building space is becoming scarce. The lack of building ground easily constructible leads to the growing use of earthwork structures. The latter allows the development of the city in the alluvial plains without considering that increasing water constriction would lead to increased flooding for some areas (e.g. Douglas et al., 2008). For the largest backfill areas associated with large costly urban project (luxury apartments, industrial complex, national road, ...), geotechnical investigation were generally carried out and subsequent foundation problems are rare. In other cases, infilling were done without any geotechnical studies and compliance to construction standard, so the risk of building collapse is high. The photos in appendix 3.B figure provides an example of this problem for the building located next to the University of Antananarivo. The case of the city of Antananarivo is similar to other large African cities that witness an

extremely rapid growth of their urban population usually unplanned and unsustainable (Cohen, 2006; Songsore, 2009; Cobbinah et al., 2009).

Finally several key information are not fully adequate or are not provided in the geotechnical map. Flood, fill and landslide areas should be given in any engineering geological map. Here we provide a very minimal estimate of the flood area, but an in-depth study hydro-geological study needs to be conducted in the area. Flooding is the largest natural risk in Antananarivo, and it depends on many factors on the plain: the state of the flood protection along the Ikopa River and of the irrigation canals, and the capacity of the pumping stations to evacuate water from the plain. This information is not available and subject to change. The location and extension of the fill areas should also be indicated, but they are not systematically known because most fill and construction work are done without proper construction permit. We could identify some using the DEM, but not systematically. Finally the evaluation of the landslide areas and landslide hazard is an other and separate research project, because a complete landslide inventory does not exist.

5. Conclusion

Geotechnical data from the underground of Antananarivo, the Capital city of Madagascar presented here attest for a typical thick regolith cover above a crystalline basement, a geological setting that is common to most of the African continent. Geomechanical properties show that this clay rich mobile cover is a weak material and is thus a challenge for an orderly urban development. The geotechnical maps, we built, used a geotechnical database assembled in a Geographical Information System, and took into account geological and geomorphological factors. Within this system, map updating with new data will be straightforward.

These geological engineering maps provide a first understanding of the strength of the underground geological material and its

geotechnical properties. A relevant geomechanical parameter, the soil bearing capacity was computed, and the bearing capacity maps obtained would allow the policy makers to directly plan with precision the extension of the city using an adequate and normalized technical knowledge. Before a new construction project, the information may be used to impose a particular layout. They would thus (1) facilitate the first phase of a secure urban planning at a reduced cost, (2) reduce inappropriate foundation building with consequent saving for the society and the economy. For the existing sites, the geotechnical maps would help understand the constructive condition, providing a tool for risk management while reducing the loss, the vulnerability, enabling the prioritization of the intervention according to the information about the site and the level of the incurred risks.

Conflicts of interest

The authors declare they have no conflict of interest.

Appendix J. Supplementary data

Supplementary data to this article can be found online at <https://doi.org/10.1016/j.jafrearsci.2018.12.003>.

Appendix I. Computation of the soil bearing capacity

A- In situ measurements

For the calculation of the bearing capacity of a foundation using the pressuremeter method, the following parameters were used: P_1 (limit pressure), the piezometric level, the dimension of the foundation and the apparent density of the soil at the anchorage level of foundation. The corrected value of P_1 is directly obtained from the pressuremeter test. The piezometric level is obtained by direct measurements from sampling using manual or mechanical auger in the prehole allowing the pressuremeter measurements. The density of soil at the foundation level is estimated according to the nature of the soil to this depth. The calculation of superficial foundations results directly from the interpretation of pressuremeter tests (Fourni, 1981).

The bearing capacity is given by the equation, $q_1 = q_0 + k(p_{1e} - p_o)$, with q_1 : Permissible constraint to the base of the foundation; q_0 : Total vertical stress at foundation level after completion of works; k : Lift factor which depends on the dimensions of the foundation, its relative embedding and the nature of the soil; p_{1e} : equivalent limit pressure; p_o : Horizontal stress at the depth of anchorage of the foundation at the time of the pressuremeter test. However, the permissible stress must be such that any risk of rupture is avoided (Philliponnat, 1979), so a factor of safety generally taken equal to 3 is used, and the resulting equation is $q_1 = q_0 + k/3 (p_{1e} - p_o)$. The vertical stress q_0 is determined according to the formula: $q_0 = g D$ with g , the density of the soil at the level of the foundation and D , the anchoring depth of the foundation. The lift factor k is taken from the abacus extracted from DTU 13.12 below:

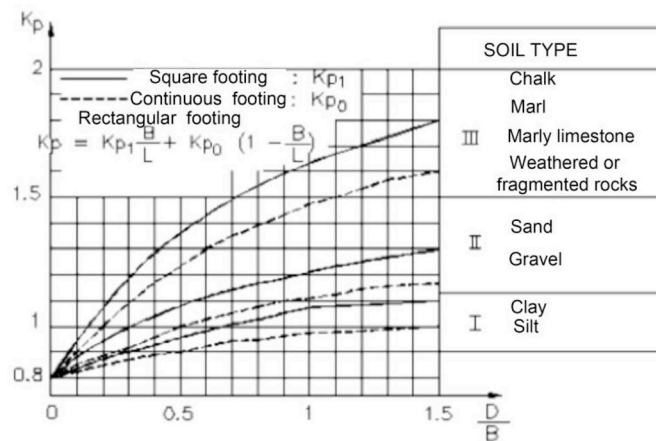


Figure. Abacus to determine the value of the lift factor k , labeled K_p in function of the type of foundation and nature of soil, with B : Foundation width; L : Foundation length; D : Foundation Anchorage depth.

The equivalent limiting pressure P_{1e} , is given by the following formula:

$$p_{1e} = \sqrt[3]{p_{l1} \times p_{l2} \times p_{l3}}$$

with p_{l1} : value of p_1 to a level located at the depth B above the level of the base of the foundation; p_{l2} : value of p_1 measured at the level of the base; p_{l3} : value of p_1 measured under the base to a depth of one width of the foundation. The horizontal stress P_o is given by the formula $P_o = u + (\sigma_{vo} - u) k_o$ where u is the water pressure at the foundation; σ_{vo} is the total vertical stress of the foundation's land at the time of the test; k_o is the coefficient of resting land ($k_o = 0.5$ in general).

Acknowledgement

S. Andriamamonjisoa is grateful to the University of Liège, where a significant part of this study was conducted with the framework of its master thesis (Master en Gestion des Risques et des catastrophes, ULiège). We thanks the two anonymous reviewer and the editor for constructive feed-back. This study was realized thanks to the help of Prof. Ramasiarino V. and Dr. Ralison A.B. from the University of Antananarivo, Tessier P. and Guyard S. from the Région Réunion, Razafindrakoto A. from the M2PATE (Ministère auprès de la Présidence chargé des Projets Présidentiels, de l'Aménagement du Territoire et de l'Équipement). We are also grateful to the engineers from the Laboratoire National des travaux publics et du bâtiment in Antananarivo that contributed significantly to the realization of this publication. Finally we thank M. El Ouhabi for her feed-back about the clay mineralogy.

B. Laboratory test

The bearing capacity for a superficial foundation from laboratory tests is given by (GEOS, 2013):

$$q'u = i_c S_c C N_c + \frac{1}{2} S_\gamma \gamma B N_\gamma i_\gamma + S_q \gamma D N_q i_q$$

i_c , i_γ and i_q are the coefficients that consider the inclination of the load on the vertical. S_c , S_γ and S_q are shape coefficients of the foundation; N_c , N_γ and N_q are dimensionless parameters whose values are defined according to the value of the internal friction angle ϕ and soil cohesion in place c (kPa); γ is the apparent weight (kN/m³). The laboratory tests give directly the values of c , ϕ and γ . The values of the coefficients taking into account the inclination of the charges are given by the formulas $i_\gamma = (1 - \theta/\phi)^2$ and $i_c = i_q = (1 - \theta/90^\circ)^2$ with θ the inclination of the load to the base of the foundation. The values of the form factors are taken from Table 5.

Table A

Values of the form factors for the calculation of bearing capacity of a superficial foundation from laboratory tests (from Ladeira et Ferreira, 1994). ϕ : internal friction angle; B: foundation width; L: foundation length.

	S_c	S_q	S_γ
Isolated footing	1.0	1.0	1.0
Rectangular footing	$1 + B/L$	$1 + (B/L) \tan \phi$	$1 - 0.4 (B/L)$
Circular footing	$1 + N_q/N_c$	$1 + \tan \phi$	0.6

The various parameters such as the lift factors N_c , N_γ and N_q are given as a function of the internal friction angle ϕ . Each value of ϕ corresponds to the values of the lift factors. Details are given in Table 6.

Table B

Lift factor for the calculation of the bearing capacity of a superficial foundation as a function of ϕ (from Ladeira et Ferreira, 1994).

ϕ	N_c	N_q	N_γ
0	5.14	1.0	0.0
5	6.5	1.6	0.5
10	8.3	2.5	1.2
15	11	3.9	2.6
20	14.8	6.4	5.4
25	20.7	10.7	10.8
30	30.1	18.4	22.4
32	35.5	23.2	30.2
34	42.2	29.4	41.1
36	50.6	37.7	56.3
38	61.4	48.9	78
40	75.3	64.2	109.4
42	93.7	85.4	155.6
44	118.4	115.3	224.6
46	152.1	152.1	330.4
48	199.3	199.3	496
50	266.9	266.9	762.9

Appendix II. Typical computation note

Bearing capacity for square insulated footing foundation (B = 1.00 m - D = 0.50 m).

Site N°30 - REF 07 SF 12

Geotechnical investigation for the construction of a laboratory at Ankatso.

Foundation: Square insulated footing.

Width B: 1.00 m

Anchorage D: 0.50 m

Computation results: Bearing capacity

Method of DTU 13.12

$P_{le}^* = 0.337$ MPa

$K_p = 0.949$

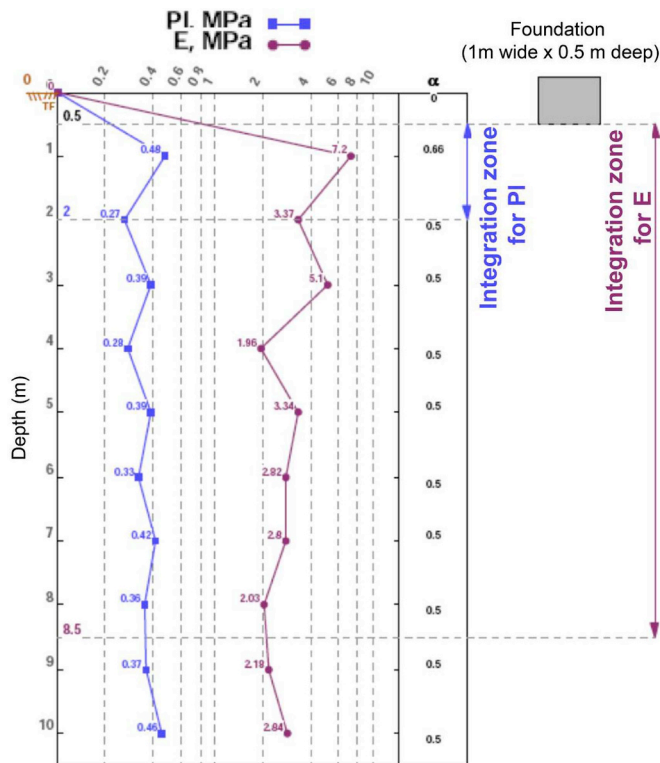
$i\delta\beta = 1$

$q'u = 0.329$ MPa

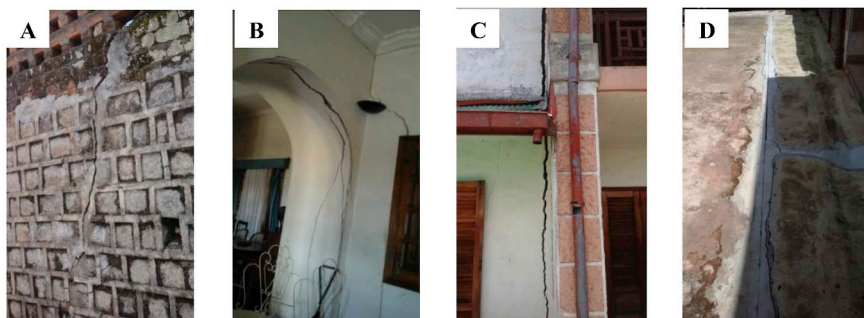
Bearing capacity (ELS) = 0.110 MPa

Bearing capacity (ELU) = 0.164 MPa

Computation input (Pl: Limit Pressure; E: Pseudo-Elastic Deformation modulus).



Appendix III. Examples of building damages due to water pipe leakage on the Roya Hills in Fig. 1 and due to the differential settlement of the embankment below the building in Fig. 2



A : Retaining wall on the southern side - B : Crack inside the building - C : Crack on the western wall of the building - D : Crack in the inner courtyard

Fig. 1 Cracking due to settling of the foundation (softening of the foundation soil under the effect of water).

A: Retaining wall on the southern side - B: Crack inside the building - C: Crack on the western wall of the building - D: Crack in the inner courtyard.



A: wall of the bedroom; B: wall of the living room; C: wall of the bathroom (1.5 cm thick and 35 cm long)

Fig. 2 Cracking inside the building due to the differential settlement of the embankment (foundation Level).

A: wall of the bedroom; B: wall of the living room; C: wall of the bathroom (1.5 cm thick and 35 cm long).

References

- Aly, M.H., Giardino, J.R., Klein, A.G., 2005. Suitability assessment for New Minia City, Egypt: a GIS approach to engineering geology. *Environ. Eng. Geosci.* 11 (3), 259–269.
- Amadi, A.N., Eze, C.J., Igwe, C.O., Okunlola, I.A., Okoye, N.O., 2012. Architect's and geologist's view on the causes of building failures in Nigeria. *Mod. Appl. Sci.* 6 (6), 31.
- Arnould, M., 1974. Problèmes de cartographie en géologie de l'ingénieur (cartographie géotechnique), centenaire de la société géologique de Belgique. colloque géologique de l'ingénieur, Liège, pp. 313–322.
- Berhane, G., Walraevens, K., 2013. Geological and geotechnical constraints for urban planning and natural environment protection: a case study from Mekelle City, Northern Ethiopia. *Environmental earth sciences* 69 (3), 783–798.
- Bourgeat, F., Ratsimbazafy, C., 1975. Retouches à la chronologie du Quaternaire continental de Madagascar. Conséquences sur la pédogenèse: *Bull. Soc. Geol. Fr.* 17, 554–561.
- Bündnis Entwicklung Hilft, 2016. Alliance development works) and united Nations university – Institute for environment and human security (UNU-EHS. *World RiskReport 2016*. p 47. <http://weltrisikobericht.de/wpcontent/uploads/2016/08/WorldRiskReport2016.pdf>.
- Bureau National de Gestion des Risques et des Catastrophes, 2015. Plan national de contingence sur les cyclones et les inondations, Version N°4. p 42. http://reliefweb.int/sites/reliefweb.int/files/resources/F4075FC9B5EF0778525783A00567EBE-Rapport_complet.pdf.
- Chaperon, P., Danloux, Y., Ferry, L., 1993. Fleuve et rivière de Madagascar, Monographie hydrologique. Edition Orstom, Paris, pp. 874 10.
- Clayton, A., 2012. Destructive Storms, Dormant Policies: the Impact of Cyclones on Food Security in Madagascar. <http://dspace.africaportal.org/jspui/bitstream/123456789/33394/1/Africa%20Portal%20Background%20No%20%2046.pdf>.
- Cobbinah, P.B., Erdiaw-Kwasie, M.O., Amoateng, P., 2015. Africa's urbanisation: implications for sustainable development. *Cities* 47, 62–72.
- Cobbinah, P.B., Erdiaw-Kwasie, M.O., Amoateng, P., 2015. Rethinking sustainable development within the framework of poverty and urbanisation in developing countries. *Environmental Development* 13, 18–32.
- Cohen, B., 2006. Urbanization in developing countries: current trends, future projections, and key challenges for sustainability. *Technol. Soc.* 28 (1–2), 63–80.
- Cox, R., Zentner, D.B., Rakotondrazafy, A.F.M., Rasoazanamparany, C.F., 2010. Shakedown in Madagascar: occurrence of lavakas (erosional gullies) associated with seismic activity. *Geology* 38 (2), 179–182.
- Culshaw, M.G., Price, S.J., 2011. The 2010 Hans Cloos lecture. *Bull. Eng. Geol. Environ.* 70 (3), 333–376.
- Dai, F.C., Lee, C.F., Zhang, X.H., 2001. GIS-based geoenvironmental evaluation for urban land-use planning: a case study. *Eng. Geol.* 61, 257–271.
- Davies, T.C., 2015. Urban geology of African megacities. *J. Afr. Earth Sci.* 110, 188–226.
- Dearman, W.R., 1991. *Engineering Geological Mapping*. Edition Butterworth-Heinemann, pp. 379.
- Delbos, L., 1960. Les granites précambriens à Madagascar. *Bull. Soc. Geol. Fr.* 7 (6), 790–795.
- Delubac, G., Rakotoarison, W., Rantoanina, M., 1963. Notice explicative sur les feuilles Tananarive Manjakandriana PQ 47. Tananarive Service Géologique. pp. 55.
- Dimuna, K.O., 2010. Incessant incidents of building collapse in Nigeria: a challenge to stakeholders. *Global J. Res. Eng.* 10 (4), 75–84.
- Douglas, I., Alam, K., Maghenda, M., McDonnell, Y., McLean, L., Campbell, J., 2008. Unjust waters: climate change, flooding and the urban poor in Africa. *Environ. Urbanization* 20 (1), 187–205.
- Ede, A.N., 2013. Building collapse in Nigeria: the trend of casualties the last decade (2000–2010). *Int. J. Civ. Environ. Eng.* 10 (6).
- El May, M., Dlala, M., Chenini, I., 2010. Urban geological mapping: geotechnical data analysis for rational development planning. *Eng. Geol.* 116 (1–2), 129–138.
- Forni, M., 1981. *Fondation et reprise en sous œuvre*. Edition Eyrolles, Paris, pp. 172.
- GEOS, 2013. *Manuel d'utilisation. Semelles et remblais, pieu et groupe de pieux, colonnes ballastées et inclusion rigide*. pp. 129.
- Gruber, G.A.G., Rodrigues, J.E., 1994. *Engineering Geological Mapping of Cosmopolis Area, Brazil: a Tool for Land Use Planning*, vol. II. University of Sao Paulo, Lisboa, Portugal, pp. 1273. Brazil, 7th international congress, international association of engineering geology.
- Gupta, A., Ahmad, R., 1999. Geomorphology and the urban tropics: building an interface between research and usage. *Geomorphology* 31 (1–4), 133–149.
- Gutiérrez, M., 2013. *Geomorphology*. CRC Press, Taylor & Francis Group, 978-0-415-59533-9pp. 1003 2013.
- Hoeblich, J., Hoeblich, J.M., 1983. Organisation du relief dans les environs de Tananarive. *Mad. Rev. de Géol.* N°43 29 juillet - décembre 1983.
- Holtz, R.D., Kovacs, W.D., 1981. *An Introduction to Geotechnical Engineering*. Prentice-Hall, Englewood Cliffs, New Jersey.
- Hrasna, M., Vlcko, J., 1994. Developments in Engineering Geological Mapping in Slovakia, 7th International Congress, vol. II. International Association of Engineering Geology, Lisboa, Portugal, pp. 1273.
- Hydretude, 2015. *Gestion des Risques d'Inondation et de Mouvement de Terrain à Antananarivo. Projet GRIMA. Application réglementaire à l'échelle d'un quartier pilote PHASE II*. pp. 131.
- Jacobs, L., Dewitte, O., Poesen, J., Maes, J., Mertens, K., Sekajugo, J., Kervyn, M., 2016. Landslide characteristics and spatial distribution in the Rwenzori Mountains, Uganda. *J. Afr. Earth Sci.* 30, 1e14.
- Jury, M.R., 2003. *The climate of Madagascar*. In: Goodman, S.M., Benstead, J.P. (Eds.), *The Natural History of Madagascar*. Chicago. University of Chicago Press, pp. 76–87.
- Kadhim, N., Ahmed, A.M., 2015. The geotechnical maps for bearing capacity by using GIS and quality of ground water for al-Imam district (Babil-Iraq). *Int. J. Civ. Eng. Technol.* 6, 176–184.
- Ladeira, F.L., Ferreira, G.L.M., 1994. *Bearing Capacity in Engineering Geological Mapping*. 7th International Congress, vol. II. International Association of Engineering Geology, Lisboa, Portugal, pp. 1273.
- Lateef, A.S.A., Fernandez-Alonso, M., Tack, L., Delvaux, D., 2010. Geological constraints to urban sustainability, Kinshasa city, democratic republic of Congo. *Environ. Geosci.* 17 (1), 17–35.
- Lemacha, H., Ghafiri, A., Bakiz, A., Soufi, A., EL Moutaki, S., 2017. Geotechnical and geophysical study of ain harrouda new city (Morocco). *J. Geol. Geophys.* 6 (312), 2.
- Madagascar, Artelia, 2014. *Elaboration du schéma directeur d'assainissement urbain du grand Tana, rapport final*. p 156. http://www.pseau.org/outils/biblio/resume.php?docum_document_id=4964.
- Martínez-Graña, A., Goy, J.L., Zazo, C., Yenes, M., 2013. Engineering geology maps for planning and management of natural parks: “Las batuecas-sierra de Francia” and “Quilamas” (central Spanish system, salamanca, Spain). *Geosciences* 3 (1), 46–62.
- Mietton, M., Razafimahefa, R., 2011. A mudslide in the Madagascar highlands (Antsirabe Region) Impartance of local site factors and climatic triggering. *Z. Geomorphol.* 55 (1), 15–30.
- Murray, H.H., 2007. *Applied Clay Mineralogy: Occurrences, Processing and Application of Kaolins, Bentonites, Palygorskite-sepiolite, and Common Clays*. Elsevier, Amsterdam.
- Nash, D.J., Pribyl, K., Klein, J., Endfield, G.H., Kniveton, D.R., Adamson, G.C., 2015. Tropical cyclone activity over Madagascar during the late nineteenth century. *Int. J. Climatol.* 35 (11), 3249–3261.
- Olatinsu, O.B., Oyedele, K.F., Ige-Adeyeye, A.A., 2019. Electrical resistivity mapping as a tool for post-reclamation assessment of subsurface condition at a sand-filled site in Lagos, southwest Nigeria. *SN Applied Sciences* 1 (1), 2.
- Oloyede, S.A., Omoogun, C.B., Akinjare, O.A., 2010. Tackling causes of frequent building collapse in Nigeria. *J. Sustain. Dev.* 3 (3), 127.
- Oyediran, I.A., Famakinwa, J.O., 2015. Geotechnical basis for building instability and failure: case study from Lagos, Nigeria. In: *Engineering Geology for Society and Territory*, vol. 5. Springer, Cham, pp. 365–370.
- Peter, A., 1969. *Essai de cartes géotechniques*. *Rev Sol-Soils* 16 (V), 13–27.
- Peuryraubes, D., 2016. La gestion du risque cyclonique à Madagascar: retour sur l'épisode "Giovanna" (février 2012). *Cyso-Géo. Géographie physique et environnement* 10, 153–169.
- Phillipponat, G., 1979. *Fondation et ouvrage en terre*. Edition Eyrolles, pp. 402.
- Rabe, H., 2012. Antananarivo dans son contexte national: quelle vision de l'Etat pour le développement urbain de la capitale malgache? Actes du séminaire international sur le développement urbain (in French). *Commune Urbaine d'Antananarivo March 2012*. <https://www.ville-developpement.org/docman-liste/download/1209/447-120921a-actes-seminaire>.
- Rajaonary, A., Rafanoharantsoa, A., 2012. Quelles directions pour le développement urbain. Maintien de l'agriculture urbaine, développement économique, équité sociale. Actes du séminaire international sur le développement urbain (in French). *Commune Urbaine d'Antananarivo March 2012*. <https://www.ville-developpement.org/docman-liste/download/1209/447-120921a-actes-seminaire>.
- Rakototsimba, A., Bettencourt, S., 2010. La gestion des risques naturels: vers une prévention renforcée et coordonnée, Madagascar: vers un agenda de relance économique. *World Bank*, pp. 364. <http://siteresources.worldbank.org/INTMADAGASCARIN/FRENCH/Resouces/GRC.pdf>.
- Raminintsoa, T., 2012. Les contraintes hydrauliques de l'urbanisation d'Antananarivo. Actes du séminaire international sur le développement urbain (in French). *Commune Urbaine d'Antananarivo Mars 2012*. <https://www.ville-developpement.org/docman-liste/download/1209/447-120921a-actes-seminaire>.
- Ramifehiarivo, N., Brossard, M., Razakamanarivo, H., 2016. Challenges in establishing digital maps of soil organic carbon in Madagascar. *Pedometron* (39), 26–31.
- Ratsimbazafy, C., 1972. Contribution à l'étude de la région centre-nord de Madagascar au niveau de Bealanana: considérations sur le lever géochimique alluvionnaire effectuée à la maille de un échantillon dans quatre kilomètres carrés (Doctoral dissertation).
- Razafimanjato, J.Y., Randriamanjakasoa, J.H., Rabeza, V.R., Rakotondrajoana, N.H., Allman, J., 2001. La situation démographique de Madagascar. *Population* 56 (4), 657–668.
- Richards, N.P., 2002. Engineering geological and geohazard mapping of the Durban Metropolitan area, Kwazulu-Natal, South Africa. In: Van Rooy, J.L., Jermy, C.A. (Eds.), *Proceedings of the 9th Congress of the International Association for Engineering Geology and the Environment*. South African Institute of Engineering and Environmental Geologists, Pretoria, Durban, pp. 725–734.
- Richards, J. (Ed.), 2009. *Mining, Society, and a Sustainable World*. Springer Science & Business Media.
- Shaaban, F., Ismail, A., Massoud, U., Mesbah, H., Lethy, A., Abbas, A.M., 2013. Geotechnical assessment of ground conditions around a tilted building in Cairo-Egypt using geophysical approaches. *J. Assoc. Arab Univ. Basic Appl. Sci.* 13 (1), 63–72.
- Songsore, J., 2009. *The Urban Transition in Ghana: Urbanization, National Development and Poverty Reduction*. University of Ghana, Legon-Accra.

- Tchamba, J.C., Bikoko, T.G.L., 2015. Failure and collapse of building structures in the cities of Yaoundé and Douala, Cameroon from 2010 to 2014. *Mod. Appl. Sci.* 10 (1), 23.
- Thomas, M.F., 1994. *Geomorphology in the Tropics*. John Wiley and Sons, Chichester, pp. 460.
- Tricart, J., 1953. Érosion naturelle et érosion anthropogène to Madagascar. *Rev. Geomorphol. Dyn.* 5, 225–230.
- Una, C.O., Igwe, O., Maduka, R., Brooks, A., Ajodo, R., Adepehin, E.J., Okwoli, E., 2015. Integrating geotechnical and geophysical techniques in assessing frequent building collapse in Akpugo, Nkanu West LGA, Enugu State, Nigeria. *Arabian Journal of Geosciences* 8 (12), 10951–10960.
- UNDESA/PD, 2012. *World Urbanisation Prospects: the 2011 Revision*. United Nations, New York.
- UNESCO, 1976. *Guide pour la préparation des cartes géotechniques*. Les presses de l'UNESCO, Association internationale de géologie de l'ingénieur, Paris, pp. 79.
- Vulliet, L., Lyesse, L., et Zhao, J., 2016. *Mécanique des sols et des roches avec écoulement souterrains et transfert de chaleur*. Presses polytechniques et universitaires romandes. *Traité de génie civil* 18, 603.